

Experimental and Numerical Study on Three Dissimilar and Two Similar Sheets Joined Using Resistance Spot Welding and Clinching Processes.

M.Tech Thesis

**By
UTKARSH SINGH**



**DEPARTMENT OF MECHANICAL
ENGINEERING
INDIAN INSTITUTE OF TECHNOLOGY
INDORE
MAY 2025**

Experimental and Numerical Study on Three Dissimilar and Two Similar Sheets Joined Using Resistance Spot Welding and Clinching Processes.

A THESIS

*Submitted in partial fulfillment of the
requirements for the award of the degree
of
Master of Technology*

by
UTKARSH SINGH



**DEPARTMENT OF MECHANICAL
ENGINEERING
INDIAN INSTITUTE OF TECHNOLOGY
INDORE
MAY 2025**

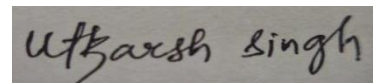


INDIAN INSTITUTE OF TECHNOLOGY INDORE

CANDIDATE'S DECLARATION

I hereby certify that the work which is being presented in the thesis entitled **Experimental and Numerical Study on Three Dissimilar and Two Similar Sheets Joined Using Resistance Spot Welding and Clinching Processes**.in the partial fulfillment of the requirements for the award of the degree of **MASTER OF TECHNOLOGY** and submitted in the **DISCIPLINE OF MECHANICAL ENGINEERING, Indian Institute of Technology Indore**, is an authentic record of my own work carried out during the time period from May 2024 to May 2025 under the supervision of Dr Ashish Rajak, Assistant professor in the department of Mechanical engineering, Indian Institute of technology Indore.

The matter presented in this thesis has not been submitted by me for the award of any other degree of this or any other institute.



Signature of the student
Utkarsh Singh 30-05-2025

This is to certify that the above statement made by the candidate is correct to the best of my/our knowledge.

Signature of the Supervisor of
M.Tech thesis
DR. ASHISH RAJAK

Utkarsh Singh has successfully given his M.Tech Oral Examination held on 26-05-2025

Signature of Supervisor of M.Tech. thesis
DR. ASHISH RAJAK
Date: 30-05-2025


Convener, DPGC
DR. S. JANAKIRAMAN
Date: 30-05-2025

ACKNOWLEDGEMENTS

I would like to express my heartfelt gratitude to my supervisors, **Dr. Ashish rajak** sir, for their invaluable guidance, expertise, and continuous encouragement. Their insightful feedback and patient mentoring have been instrumental in shaping the direction of this thesis.

I extend my sincere appreciation to the faculty members of Indian Institute of Technology, Indore for their commitment to education and their willingness to share their knowledge. Their lectures and discussions have enriched my understanding of the subject matter.

I am indebted to my family and friends for their constant encouragement and understanding. Their unwavering support, love, and belief in me have been my driving force through my research Journey.

I express my gratitude to **Mr. Ummmed Singh, Mr. Rakesh Kumar Mishra, Mr. Manoj Kumar Kushwaha, Mr. Setu Suman, Mr. Ashok Kumar, Mr. Arun Kumar Singh, and Mr. Rajendra Goud** actively participated in my research, generously sharing their insights and time. Their contributions have enriched the depth and quality of my study.

I am grateful to **IIT Indore** for granting me permission to conduct this research and for providing the necessary facilities. I would like to acknowledge the **Head of Department of Mechanical Engineering** and the **DPGC convener** for their assistance, facilities, moral support, and kindness throughout my MTech program.

They deeply appreciate the assistance and technical support provided to me at Mechanical Workshop at IIT Indore from **Dr. Anand Petare and his team of Machine Operators at workshop** in accessing resources and navigating technical challenges while building components for carrying out research work.

DEDICATION

This thesis is dedicated to all those whose support, guidance, and encouragement made this work possible.

To the family and friends who stood by throughout this journey thank you for the patience during long hours, the encouragement during moments of doubt, and the strength provided during difficult phases. Your steady presence made each challenge easier to face.

To the mentors and academic advisors whose feedback, suggestions, and direction helped shape the quality and clarity of this research your involvement was crucial to the learning process and the final outcome of this work.

To the teachers and staff who made resources and knowledge accessible at every stage, and to the classmates and peers who shared ideas and perspectives every contribution has been deeply valued.

This work is also dedicated to all learners and researchers who continue to pursue knowledge and solutions. May it stand as a reminder that progress comes with effort, persistence, and support from others.

Utkarsh Singh

Abstract

The automotive industry is increasingly adopting advanced techniques to meet the demanding performance requirements of structural components. Resistance Spot Welding (RSW) is a widely used method that joins materials using pressure and heat from an electric current. This study investigates RSW performance on a three-sheet stack-up of 0.8 mm thick stainless steel 304, galvanized iron (GI), and mild steel 1006. Welding time was varied while keeping squeeze and hold times constant. Tensile testing and cross-sectional analysis showed that joint strength improved with welding time up to 700 ms, beyond which strength declined. The best performance was achieved with stainless steel on top, mild steel in the middle, and GI at the bottom. Future work will optimize additional parameters and analyse nugget formation.

This research also explores a hybrid joining technique that combines RSW with mechanical clinching for mild steel 1006. The hybrid approach merges the rapid heating of RSW with the cold-forming interlock of clinching, enhancing joint strength, durability, and fatigue resistance. LS-DYNA simulations modelled both processes and were validated by experimental data. Tensile, shear, and fatigue tests confirmed that the hybrid method outperforms traditional techniques, offering better strength, a smaller heat-affected zone, and improved manufacturing efficiency ideal for automotive and structural applications.

TABLE OF CONTENTS

| | |
|---|----|
| ACKNOWLEDGEMENTS | |
| DEDICATION | |
| ABSTRACT | |
| LIST OF FIGURE | |
| LIST OF TABLE | |
| | |
| Chapter 1: Introduction | 1 |
| 1.1 Resistance spot welding process | 2 |
| 1.2 Mechanical Clinching process | 3 |
| 1.3 Research objectives | 3 |
| 1.4 Scope of the study | 4 |
| 1.5 Organization of the Thesis | 4 |
| Chapter 2: Fundamental Concept and Literature review | 5 |
| 2.1 Background | 5 |
| 2.2 Process of resistance spot welding | 5 |
| 2.3 Parameters affecting spot welding | 6 |
| 2.4 Types of electrode geometry | 7 |
| 2.5 Types of failure modes | 8 |
| 2.6 Defects in resistance spot welding | 9 |
| 2.7 Joining of galvanized steel with dual-phase steel sheet using the resistance spot welding process | 11 |
| 2.8 Joining of mild steel and stainless steel sheet using resistance spot welding | 12 |
| 2.9 Simulation analysis of the resistance spot welding | 12 |

| | |
|--|----|
| 2.10 Process of clinching | 13 |
| 2.11 Parameters of clinching | 14 |
| 2.12 Types of die used in clinching | 15 |
| 2.13 Types of fracture in clinching | 16 |
| 2.14 Joining of galvanized mild steel to 5083 aluminum alloy using a combined clinching & spot welding process | 18 |
| 2.15 Joining of aluminium alloy and mild steel sheet using mechanical clinching | 19 |
| 2.16 Simulation analysis of the clinching process | 20 |
| 2.17 Conclusion from literature survey | 21 |
| Chapter 3: Research methodology | 22 |
| 3.1 Experimental procedure for three-sheet resistance spot welding process | 22 |
| 3.2 Experimental procedure for two-sheet spot welding and clinching process | 25 |
| 3.3 Mechanical testing and characterization instruments | 28 |
| Chapter 4: Numerical Simulation | 29 |
| 4.1 Simulation study of three-sheet resistance spot welding | 29 |
| 4.2 Simulation study of two-sheet resistance spot welding | 30 |
| 4.3 Simulation study of two-sheet mechanical clinching | 31 |
| Chapter 5: Result and Discussion | 32 |
| 5.1 Joining of three dissimilar (SS 304, MS 1006, and GI) sheet of thickness 0.8 mm using resistance spot welding. | 32 |
| 5.1.1 Effect of pressure on lap shear test | 33 |
| 5.1.2 Effect of welding time on tensile strength | 34 |
| 5.1.3 Effect of various combination of three sheet on tensile strength | 35 |

| | |
|---|----|
| 5.1.4 Peel test | 37 |
| 5.1.5 Cross-section analysis of weld nugget in three-dissimilar sheet spot welding | 38 |
| 5.1.6 Energy dispersive spectroscopy analysis on three-sheet spot welding | 40 |
| 5.2 Joining of two mild steel (MS 1006) sheet of thickness 0.8 mm using resistance spot welding and clinching process | 42 |
| 5.2.1 Effect of welding pressure on lap-shear strength | 43 |
| 5.2.2 Effect of welding time on lap-shear strength | 44 |
| 5.2.3 Effect of clinching pressure on lap-shear strength | 46 |
| 5.2.4 Lap shear test | 47 |
| 5.2.5 Peel test | 48 |
| 5.2.6 Microstructure analysis of nugget formation in resistance spot welding | 49 |
| 5.2.7 Microstructure analysis on the effect of RSW assisted clinch joint | 51 |
| 5.2.8 Microstructure analysis on the effect of clinching-assisted RSW | 52 |
| 5.2.9 Scanning electron microscopy analysis | 53 |
| 5.2.10 Energy dispersive spectroscopy analysis on two-sheet spot welding | 55 |
| 5.2.11 Numerical analysis of spot welding on three 0.8 mm SS-MS-GI sheets | 57 |
| 5.2.12 Numerical analysis of spot welding on two 0.8 mm MS sheets. | 58 |
| 5.2.13 Numerical analysis of mechanical clinching on two 0.8 mm MS sheets. | 60 |
| Chapter 6: Conclusion and future directions | 62 |
| 6.1 Summary of findings | 62 |
| 6.2 Implications and significance | 63 |
| 6.3 Limitation and future research | 64 |
| 6.4 Recommendations for Further Study | 65 |

LIST OF FIGURES

| | |
|-----------|--|
| Figure 1 | Resistance spot welding cycle [1] |
| Figure 2 | Different electrode geometry [1] |
| Figure 3 | Different failure mode [1] |
| Figure 4 | Expulsion occurring at the faying surface [2] |
| Figure 5 | Shrinkage void at weld nugget [2] |
| Figure 6 | Solidification crack at the transition region from HAZ to base metal [2] |
| Figure 7 | Weld nugget and weld penetration [3] |
| Figure 8 | Spot welded mild steel and stainless-steel metal sheets [4] |
| Figure 9 | (a) The mechanism diagram of optimization measures (b) 2D axisymmetric FE model [5] |
| Figure 10 | Clinching process [6]. |
| Figure 11 | Cross-sectional view of clinched joint [6] |
| Figure 12 | Clinched joints and die [7] |
| Figure 13 | Neck fracture mode of the clinched joint [8] |
| Figure 14 | Hybrid neck fracture mode of the clinched joint [8] |
| Figure 15 | Hybrid button separation mode of the clinched joint [8] |
| Figure 16 | Button separation mode of the clinched joint [8] |
| Figure 17 | (a) Resistance punch and die electrode (b) Cross-section of clinch-resistance spot welding |
| Figure 18 | Deformation behavior of sheets in clinching [10]. |
| Figure 19 | Axis symmetric 2d setup for clinched joint of dissimilar sheet [11] |
| Figure 20 | Schematic setup of the RSW machine (a) Complete setup of the machine (b) Enlarged view of the working zone (c) Air compressor used in the welding process. |

| | |
|-----------|--|
| Figure 21 | Dimension of samples (a) before spot welding (b) after spot welding |
| Figure 22 | (a) Schematic setup of the clinching machine (a) Complete setup of the machine (b) Enlarged view of the working zone (c) Air compressor used in the clinching process. |
| Figure 23 | Dimensions of the sample prepared for mechanical clinching |
| Figure 24 | Two different types of electrodes used (a) punch and die type actual (b) pointed type actual (c) punch and die dimension (d) pointed type dimension. |
| Figure 25 | Axis symmetric 2d simulation setup for spot welding of three-sheet |
| Figure 26 | Axis symmetric 2d simulation setup for spot welding of two sheets |
| Figure 27 | Axis symmetric 2d simulation setup for clinching of two sheets |
| Figure 27 | Arrangement made for 3 sheet mechanical tests (a) lap-shear test (b) Peel test. |
| Figure 28 | (a) Failed sample after lap shear test, (b) Result of the lap shear test for various pressure. |
| Figure 29 | (a) Failed sample after lap shear test, (b) Result of the lap shear test for various weld time. |
| Figure 30 | Failed sample after lap shear test, (b) Result of the lap shear test for various three sheet-combination |
| Figure 31 | Failed sample after peel test, (b) Result of the peel test.. |
| Figure 32 | Weld nugget geometry analysis for various combination of sheets |
| Figure 33 | EDS analysis on (a) area of three sheet spot welding (b) mapping on three sheet spot welding. |
| Figure 34 | Arrangement made for 2 sheet mechanical tests (a) lap-shear test (b) Peel test. |
| Figure 35 | (a) Failed sample after lap shear test, (b) Result of the lap shear test for various pressure. |
| Figure 36 | (b) Failed sample after lap shear test, (b) Result of the lap shear test for various weld time. |
| Figure 37 | (a) Failed sample after lap shear test, (b) Result of the lap shear |

| | |
|-----------|---|
| | test for various clinching pressure |
| Figure 38 | Failed sample after lap shear test (a) Spot welding assisted clinch joint (b) clinching assisted spot welding (c) Result of the lap shear test. |
| Figure 39 | Failed sample after peel test (a) Spot welding assisted clinch joint (b) clinching assisted spot welding (c) Result of the peel test. |
| Figure 40 | (a) Mild steel sheet nugget zone (b) base metal (c) near HAZ (d) Fusion zone (d) Opposite of heat affected zone. |
| Figure 41 | (a) Cross-sectional view of RSW assisted clinch joint, (b) 20x – 50 μm (scale), (c) 50x – 20 μm (scale), (d) 50x – 20 μm (scale), and (e) 100x – 10 μm (scale) |
| Figure 42 | (a) Cross-sectional view of clinching assisted RSW joint, (b), (c) 10x – 100 μm (scale), (d) 20x – 50 μm (scale), and (e) 50x – 20 μm (scale) |
| Figure 43 | View of RSW-assisted clinch joint (a) Clinching centre region, (b) Enlarged view of clinching centre region, (c) Clinching neck thickness region, and (d) Enlarged view of clinching neck thickness region |
| Figure 44 | View of Clinching assisted RSW joint (a) Clinching centre region, (b) Enlarged view of clinching centre region, (c) Clinching neck thickness region, and (d) Enlarged view of clinching neck thickness region |
| Figure 45 | EDS analysis on (a) area of two sheet spot welding assisted clinching (b) mapping on two sheet spot welding assisted clinching. |
| Figure 46 | Fringe pattern of three dissimilar steel sheet nugget formation |
| Figure 47 | Fringe pattern of three dissimilar steel sheet current density variation |
| Figure 48 | Fringe pattern of two mild steel sheet nugget formation |
| Figure 49 | Fringe pattern of two mild steel sheet current density variation |
| Figure 50 | Fringe pattern (a)Two mild steel sheet plastic strain variation (b) Two mild steel sheet von-mises Stress variation |

LIST OF TABLES

| | |
|----------|---|
| Table 1 | Mechanical properties of the materials used in the three-sheet experiment. |
| Table 2 | Mechanical properties of the materials used in the two-sheet experiment |
| Table 3 | Optimization of pressure parameters for three-sheet spot welding |
| Table 4 | Optimization of weld time parameters for three-sheet spot welding |
| Table 5 | Optimization of different material sheet combination for three-sheet spot welding |
| Table 6 | Peel test result for three-sheet spot welding |
| Table 7 | Optimization of pressure parameters for two-sheet spot welding |
| Table 8 | Optimization of weld time parameters for two-sheet spot welding |
| Table 9 | Optimization of pressure parameters for two-sheet mechanical clinching |
| Table 10 | Lap shear test result for spot welding-assisted clinch joint |
| Table 11 | Lap shear test result for clinch joint-assisted spot welding |
| Table 12 | Peel test result for spot welding-assisted clinch joint |
| Table 13 | Peel test result for clinch joint-assisted spot welding |

Chapter 1

Introduction

Resistance spot welding (RSW) is a common welding method that joins two or more metal sheets by applying focused heat and force, created through electrical resistance. In this method, electric current flows through the metals, which heat up because of their resistance to the electric flow. The generated heat melts the interface point, and when combined with force, the materials bond together, forming a unified joint. RSW is heavily used in fields like automobile production, especially for assembling steel sheets in body panels, and in building electric parts, appliances, and air-frame elements. Its productivity, speed, and capacity to join mixed metals make it a key process for mass production lines.

Clinching is a method for joining sheets broadly used in many industries, allowing parts to be connected without needing added materials like adhesives or fillers. This process joins sheets by pressing them to deform and create a solid lock through mechanical interlocking. It is well-suited for combining metals that are tough to weld or have coatings that would suffer from normal joining techniques. Clinching is frequently used in sectors like auto, aerospace, electronics, and appliances, for making housings, fixing chassis, and assembling units. Thanks to its many strengths and wide range of compatible materials, clinching stays a trusted method for joining sheets in current production settings. It reduces energy use since no heating is required and minimizes tool wear over long production runs. Clinching also supports automation, making it suitable for continuous and cost-effective manufacturing processes..

Advantages of resistance spot welding process :-

1. RSW is a fast process, making it ideal for high-volume production, especially in industries like automotive manufacturing.
2. Unlike other welding methods, RSW does not require additional materials such as filler metals or flux, reducing costs and simplifying the process.

3. RSW can join a variety of materials, including steel, aluminium, and copper, and is particularly useful for joining dissimilar metals.
4. The process generates less waste compared to other methods, as there is no need for additional materials or coatings.

Advantages of the clinching process :-

1. Clinching creates strong mechanical interlocks between metal sheets, resulting in durable, reliable joints capable of withstanding various mechanical stresses.
2. Unlike traditional welding or adhesive bonding methods, clinching does not require filler materials, adhesives, or consumables, which reduces material costs.
3. Compared to other joining methods like welding, clinching requires less energy, making it a more energy-efficient process.
4. The process is adaptable to a wide range of materials, including various metals, and can be used to join materials of differing thicknesses and types.

1.1 Resistance spot welding process

It is a method of joining two or more metal sheets by applying pressure and generating heat through electrical resistance. The heat needed for welding is produced by Joule heating, where heat (Q) depends on current (I), resistance (R), and time (t). This technique does not require any additional filler material and can effectively join different types of metals. It is also an eco-friendly process and is well-suited for welding multiple layers.

The process parameters that affect spot welding are weld current, electrode force, and electrode geometry. Soomro et al. have used different types of electrodes in spot welding. Those are pointed (type A), dome (type B), flat (type C), offset (type D), truncated (type E), and radius (type F) [1] and observed that the performance of type A of the electrode was better among the all different types of electrodes.

1.2 Mechanical clinching process

Clinching joins two sheets through plastic deformation and is classified as a cold-forming technique. This process is very quick, requiring minimal time to create a joint. It does not need any extra filler material, making it simple to use. Clinching also allows easy joining of dissimilar materials, demands low maintenance, and helps minimize material waste. Four different stages exist in the clinching process and the phases that exist are the positioning phase, extrusion phase, deformation phase, and interlock phase.

1.3 Research objectives

The main aim of this M. Tech thesis is to thoroughly study the joining of a layered assembly made up of 0.8 mm thick sheets of SS 304, MS 1006, and GI through resistance spot welding. Additionally, the research investigates the joining of two mild steel sheets (0.8 mm thick) using the mechanical clinching technique. The study centers around the following important objectives:

- Experimental study on 0.8 mm thick SS 304, MS 1006, and GI dissimilar sheets joined using resistance spot welding.
- Characterization of 0.8 mm thick SS 304, MS 1006, and GI dissimilar sheets joined using resistance spot welding.
- Experimental study of clinch-assisted spot welding and spot-assisted clinch joint of two similar 0.8 mm MS sheets.
- Characterization of clinch-assisted spot welding and spot-assisted clinch joint of two similar 0.8 mm MS sheets.
- Finite element simulation of spot welding for both three-sheet dissimilar metal joints and two-sheet similar metal joints, along with clinch joining of dual 0.8 mm mild steel layers.

1.4 Scope of the study

To achieve the research objectives, 2D simulations of the clinching and resistance spot welding processes will be performed using LS-DYNA. Lap shear and peel tests will evaluate joint strength, while digital and optical microscopy will analyze cross-sections for weld quality and the effects of varying welding times. Combining simulation and experiments, this study aims to provide detailed insight into the mechanical behavior and structural integrity of different joining methods, supporting practical applications in multi-material engineering.

1.5 Organization of the Thesis

This thesis is structured into several chapters to present the research findings and analysis in a clear and systematic way. Chapter 2 provides a comprehensive review of the existing literature, explaining the fundamental concepts of clinching and resistance spot welding for two-sheet stacks, as well as resistance spot welding for three-sheet stacks. It also includes a review of earlier studies that are relevant to this work. Chapter 3 outlines the research methodology, detailing the experimental arrangement, the materials selected, and the testing methods followed. Chapter 4 highlights the numerical study and 2D simulations related to the resistance spot welding and mechanical clinching processes. Chapter 5 provides the experimental findings, including test results and microstructural analysis of the welded and clinched samples. Lastly, Chapter 6 concludes the thesis by summarizing the key research outcomes and offering recommendations for future research directions in this field.

In summary, this M.Tech thesis delivers meaningful insights into the joining of three-layer sheet assemblies through resistance spot welding, as well as two-layer joints using both RSW and clinching methods. The outcomes contribute to the understanding of lightweight, multi-material joints with practical importance in diverse engineering applications.

Chapter 2

Fundamental Concept and Literature Survey

2.1 Background

RSW is a commonly used industrial method for joining metal sheets by producing heat through Joule heating ($J = I^2Rt$) [1]. During this process, copper or copper alloy electrodes cooled by water are placed on either side of the sheets. These electrodes apply force to clamp the sheets together and simultaneously pass electric current through them, resulting in localized melting that creates the weld joint.

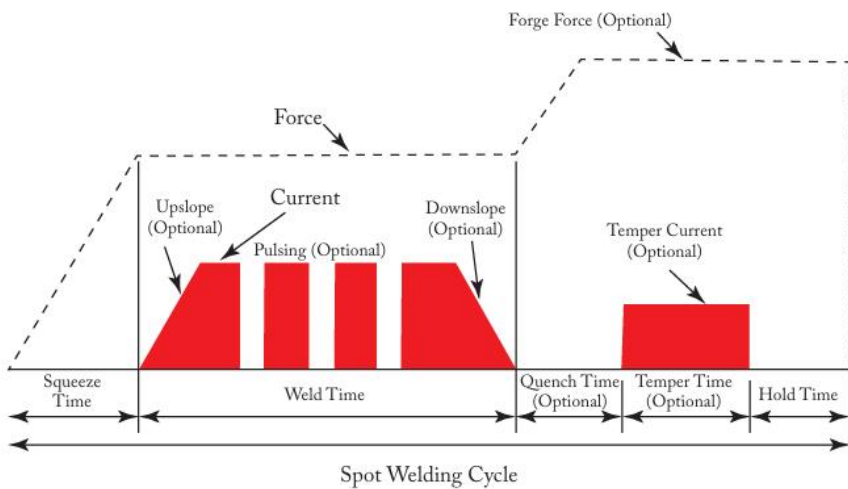


Figure 1 Resistance Spot welding Cycle [1]

2.2 Process of resistance spot welding

(a) Squeeze time - This initial phase of the welding cycle involves the electrodes pressing against the metal sheets to secure them in place. Its main objective is to ensure proper alignment and firm contact between the sheets before the flow of electrical current begins. This stage spans from the point of electrode contact up to the start of current application.

(b) Weld time - Once sufficient pressure secures the sheets, the electric current is activated. In this short interval, a high-intensity current passes through the metal sheets, generating heat at the interface due to electrical resistance. This heat melts the material locally, allowing a weld nugget to form as the metals bond. Excessive current duration, however, can introduce welding flaws or degrade joint quality.

(c) Hold time - After the current is switched off, the electrodes maintain pressure briefly to let the molten weld zone cool down and solidify. This holding phase is crucial for the weld to properly form and develop strong mechanical properties.

(d) Off time - In this last phase, the electrodes release the applied pressure and move back to their starting position, with no current passing through. This step resets the equipment, making it ready for the next welding operation.

2.3 Parameters affecting spot welding

(a) Weld current – Weld current is the flow of electricity that travels through metal sheets in spot welding, playing a key role in determining the amount of heat produced at the contact surface. Using a higher current helps in forming a solid weld nugget, but excessive current can result in overheating or defects, while insufficient current may cause incomplete or weak welds.

(b) Electrode force – Electrode force refers to the applied pressure that clamps metal sheets together during the welding process. This force ensures firm contact between the sheets, lowers electrical resistance at the interface, and aids in regulating heat input. Insufficient force may result in poor weld strength, while excessive pressure can distort the materials. Applying the correct amount of force is crucial for creating durable and flaw-free weld joints.

(c) Electrode geometry – The geometry of an electrode its shape and dimensions plays a key role in directing heat and electrical current during welding. A smaller tip concentrates heat into a tighter area, allowing for deeper fusion, whereas a broader tip distributes heat over a larger surface, producing wider weld spots. Using worn or unsuitable electrodes may result in irregular weld quality. Selecting the proper electrode shape is essential for achieving strong, consistent welds and extending tool life.

2.4 Types of electrode geometry

- (a) **Pointed electrode** - This electrode features a pointed or tapered end and is typically applied in welding small components or locations that are difficult to access. Its design allows electrical current to focus on a narrow spot, quickly producing intense heat. Despite its efficiency, this type tends to wear out more rapidly and might not perform well with thicker workpieces.
- (b) **Dome electrode** - Electrodes with a dome-shaped tip feature a rounded surface that ensures uniform pressure distribution over the weld zone. They are widely applied in standard welding operations due to their balanced performance in current conduction and contact area. The curved tip also helps minimize indentation on the sheet surface.
- (c) **Flat electrode** - This electrode features a broad, flat tip that distributes electrical current and force over a wider surface area. It is ideal for welding thicker metal sheets or materials that require gentle handling to prevent surface harm. However, compared to pointed electrodes, it produces less concentrated heat.
- (d) **Offset electrode** - Offset electrodes are designed with the tip positioned away from the central axis of the electrode body. This configuration is useful for welding near edges or in confined areas where standard straight electrodes are ineffective. It offers improved adaptability for various joint layouts and positioning requirements.
- (e) **Truncated electrode** - This type features a cone-shaped tip that is cut off flat at the end. It provides a focused yet slightly broader contact area than a pointed tip. Truncated electrodes are widely used in production welding as they offer good heat concentration and durability.
- (f) **Radius electrode** - Radius electrodes have a curved or rounded edge at the tip, designed to reduce indentation and wear on both the electrode and the work-piece. They're ideal for materials that require gentle pressure and minimal surface marking, such as coated or soft metals.

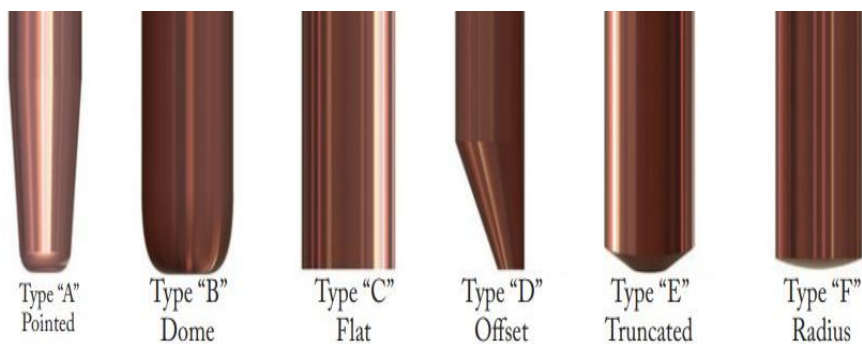


Figure 2 Different electrode geometry [1]

2.5 Types of failure modes.

(a) Button pull out - In this failure mode, the welded metal button (or nugget) remains intact and is pulled out from one of the sheets during a mechanical test like a tensile or peel test. This is usually seen as a good failure mode because it shows that the weld nugget was strong and fused properly with the surrounding metal.

(b) Partial interfacial failure - This happens when the weld breaks partially along the original interface where the sheets were joined. It indicates that the weld did not form completely across the entire contact area, possibly due to low heat.

(c) Full interfacial failure - In this case, the weld fails entirely along the interface between the sheets. The two sheets separate cleanly at the contact point without any metal pulling out. This usually suggests that the weld nugget did not form properly, and the joint is weak or defective.

(d) Partial dome failure - This occurs when the dome-like shape formed during welding begins to crack or separate, but only partially. It suggests that while some bonding occurred, it was not strong or uniform enough across the weld area, possibly due to improper force or alignment.

(e) Total dome failure - This is a complete failure of the weld dome structure. The welded joint separates entirely, often accompanied by visible deformation or cracking of the dome-shaped area. It indicates a serious welding flaw, often due to excessive heat, misalignment, or weak material properties.

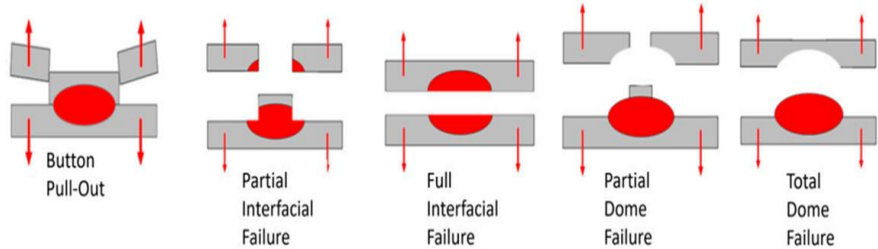


Figure 3 Different failure modes [1]

2.6 Defects in resistance spot welding.

(a) Expulsion - Expulsion happens when molten metal is forcibly ejected from the weld zone during welding. This occurs when too much heat is generated, often due to excessive welding current or poor clamping pressure. The expelled metal can create sparks or droplets, reducing weld strength and leading to inconsistent joints or material loss.

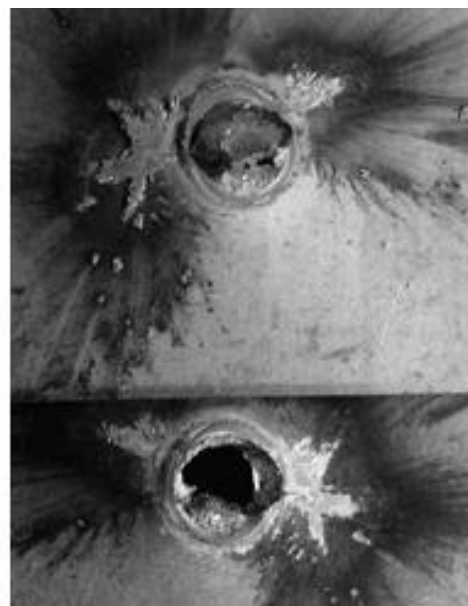


Figure 4 Expulsion occurrence at the faying surface [2]

(b) Shrinkage Void - A shrinkage void is a small cavity or empty space left inside the weld nugget as it cools and contracts. These voids form when the molten metal solidifies unevenly and doesn't completely fill the joint. They weaken the weld by reducing its density and can act as starting points for cracks under stress.

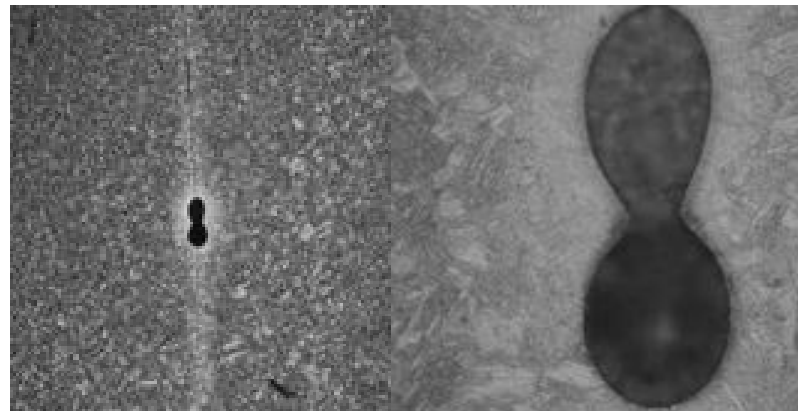


Figure 5 Shrinkage void at weld nugget [2]

(c) Solidification Crack - This type of crack forms while the weld nugget is cooling and solidifying. If the metal contracts too quickly or unevenly, it can crack along the weld line. Solidification cracks are dangerous because they may not be visible on the surface but can significantly lower the strength and durability of the weld.

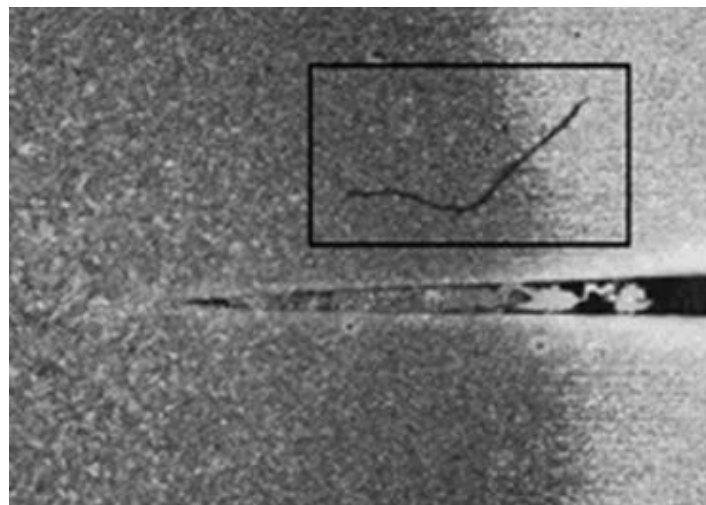


Figure 6 Solidification crack at the transition region from HAZ to base metal [2]

2.7 Joining of galvanized steel with dual-phase steel sheet using the spot welding process

Jie Shen et al [3] conducted a comprehensive study on modelling resistance spot welding (RSW) for joining multiple steel sheets commonly used in the automotive industry. They focused on welding two galvanized steel sheets (0.6 mm and 1.8 mm) with a 1.4 mm-thick Dual-Phase (DP600) steel sheet. Given the widespread use of multi-layer welding in vehicle body structures, the study aimed to better understand weld behaviour by developing a simulation model that accurately replicates the real welding process.

A key finding was that weld nugget formation occurs more rapidly in DP600 steel due to its distinct thermal and electrical properties, leading to improved weld quality and reduced energy consumption. The simulation outcomes were verified through experiments, confirming the reliability of the model. The researchers found that an optimal thickness ratio between the top and bottom sheets of about 1:3 is crucial for producing strong welds, providing key guidance for designing layered joints in automotive applications. The study emphasized the need for precise control over welding parameters such as current, pressure, and duration, since improper settings can result in weak welds or defects. Overall, these findings offer important recommendations for improving RSW processes in complex multi-layer assemblies. The work offers valuable guidelines for optimizing RSW in complex multi-stack assemblies.

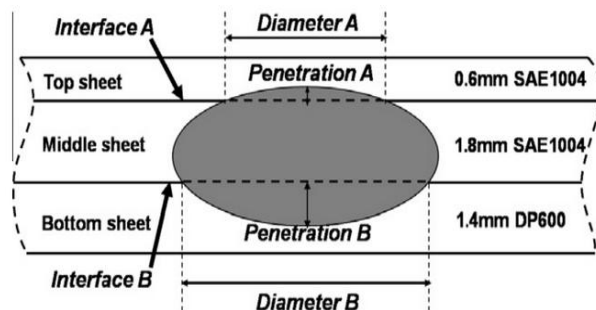


Figure 7 Weld nugget and weld penetration [3]

2.8 Joining of mild steel and stainless-steel sheet using resistance spot welding

Debashish Mishra et al [4] conducted a study on resistance spot welding (RSW) to effectively join mild steel and stainless-steel sheets, aiming to optimize the weld nugget size for enhanced joint strength. The study systematically adjusted critical welding parameters such as current, electrode pressure, and weld duration to evaluate their effects on weld quality. Results showed that higher welding current and longer weld time typically produced larger nugget sizes, which were linked to enhanced tensile shear strength of the joints. However, too much heat input led to defects like expulsion and electrode indentation, emphasizing the importance of careful control over welding conditions. The research also distinguished various failure modes, including interfacial and pullout failures, with pullout failures being more desirable due to greater energy absorption and joint durability. These outcomes offer important guidance for optimizing RSW settings when joining dissimilar metals, especially in applications demanding strong and reliable joints.



Figure 8 Spot welded mild steel and stainless-steel metal sheets [4]

2.9 Simulation analysis of the resistance spot welding process

Kang Zhou and colleagues carried out research aimed at improving the resistance spot welding (RSW) technique for joining aluminum and steel sheets, a process complicated by the distinct physical characteristics of the two metals. They analysed the dynamic resistance changes during welding and identified three distinct stages: no nugget, aluminium nugget, and aluminium/steel double nugget formation. To improve weld quality, they proposed two optimization strategies: increasing the surface roughness at the metal interface and replacing traditional flat electrodes with spherical ones. These modifications led to larger and more uniform weld nuggets, improved the spreading of molten aluminium on steel, and

reduced the formation of brittle inter-metallic compounds. Experimental results showed significant improvements in joint strength, with tensile-shear strength increasing by up to 81%. This research provides valuable insights for optimizing RSW processes in applications requiring reliable aluminium-steel joints

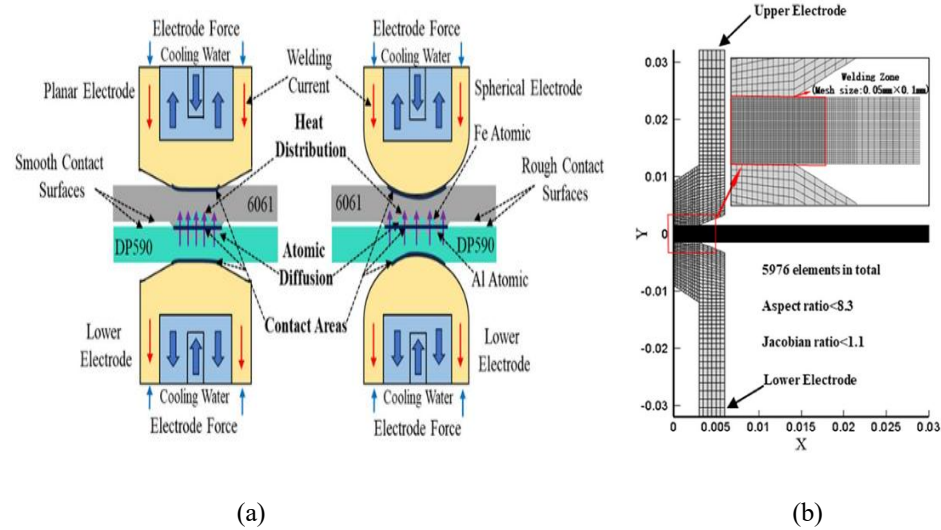


Figure 9 (a) The mechanism diagram of optimization measures (b)
2D axisymmetric multi-physics FE model [5]

2.10 Process of clinching.

Clinching is a mechanical process for joining metal sheets using a punch, die, and blank holder. The shape and strength of the joint depend heavily on the tool design. To save time and cost, simulations like finite element analysis are used to optimize these tools. This study reviews existing research on clinching simulations, highlighting challenges, parameter optimization, and factors that influence joint strength and reliability.

Generally, the clinching process contains four basic steps :-

(a) Positioning phase - In this initial step (a), the metal sheets to be joined are accurately aligned one over the other. They are then placed between the punch and the die of the clinching tool. Proper positioning is critical to ensure uniform and reliable joint formation.

(b) Extrusion phase - The punch begins to press downward (b) applying force to the upper sheet. This force causes the material to flow into the die cavity. The flow initiates the shaping of the joint without cutting or breaking the material.

(c) Deformation phase - As the punch continues to descend (c), the material undergoes plastic deformation. The die shape directs the metal flow, forming a button-like structure. This deformation is localized, maintaining the integrity of surrounding material.

(d) Interlock phase - At the end of the stroke (d), the material from both sheets flows laterally and interlocks. This interlocking creates a mechanical connection strong enough to hold the sheets together.

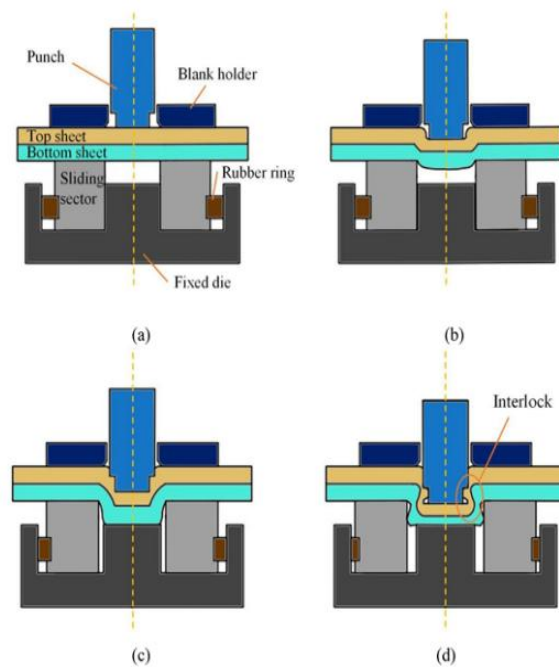


Figure 10 Clinching process [6]

2.11 Parameters of clinching

(a) Interlock - Interlock refers to the region where the materials are plastically deformed and mechanically joined during the clinching process. As the punch forces material into the die, it creates a characteristic S-shaped profile on the underside of the joint. This feature securely locks the sheets together, and the interlock's size and precision directly influence the joint's mechanical strength and reliability.

(b) Neck thickness - Neck thickness, sometimes called flange thickness, is the remaining thickness of the sheet material at the narrowest section after clinching. It forms the connection between the interlocked portion and the surrounding sheet. This dimension plays a critical role in the durability of the joint-greater neck thickness usually leads to higher joint strength but also demands increased forming force.

(c) Final bottom thickness - Final bottom thickness denotes the combined thickness of the sheets in the deformed area after the clinching operation. This thickness results from the compression and shaping of the sheets during the joining process. It helps assess the effectiveness of the clinch and can influence both joint integrity and material compatibility.

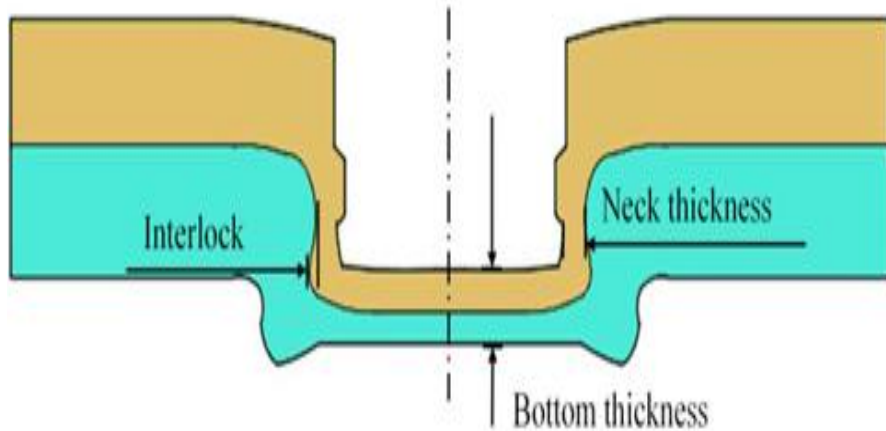


Figure 11 Cross-sectional view of clinched joint [6]

2.12 Types of die used in clinching

(a) Fixed die - A fixed die, as shown in figure 12(a), is a die that remains stationary during the clinching process. It is designed to provide a stable base for the material to be deformed against. This type of die is essential for forming a consistent joint without the need for movement or adjustment during the process.

(b) Extensible die with 2 movable segments - An extensible die consisting of two adjustable segments, shown in figure 12(b), has a design that allows the die to extend in two parts, providing increased flexibility for forming the clinched joint. These movable segments can be adjusted to fit various thicknesses or joint setups. This flexibility improves both the accuracy and adaptability of the clinching operation.

(c) Extensible die with 3 movable segment – An extensible featuring three adjustable segments, shown in figure 12(c), allows for even more flexibility by adding an additional segment. These three movable component allows the die to accommodate a wider range of material types and joint designs. The design enhances control during the forming process, leading to more consistent joint strength.

(d) Extensible die with 4 movable segment - An extensible die with 4 movable segments offers the highest level of adjustability, allowing for precise control over the deformation of the material. With four segments, the die can handle complex geometries and different material thicknesses, ensuring a reliable and strong joint formation. This die design is particularly useful for advanced clinching processes requiring high precision.

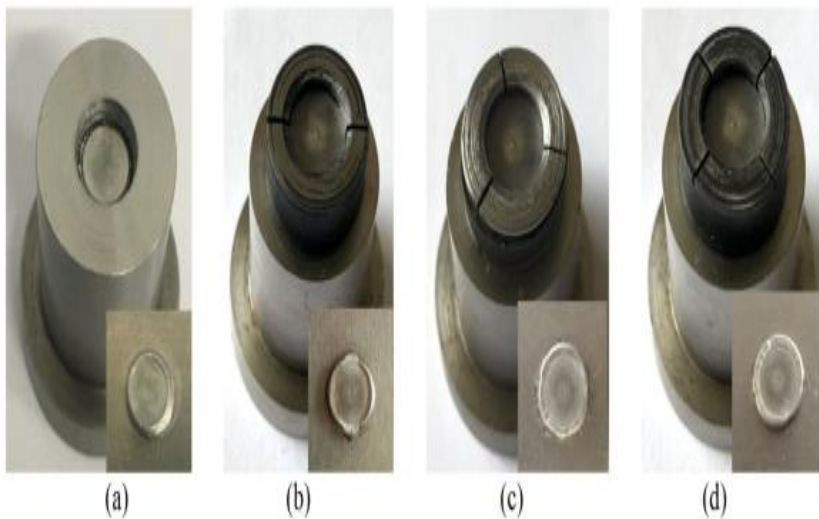


Figure 12 Clinched joint and die [7]

2.13 Types of fracture in clinching

(a) Neck fracture - This failure mode occurs when the material at the neck the thinnest part of the upper sheet-breaks due to tensile forces. It typically indicates that the material could not withstand the stress concentration created during loading, leading to a clean fracture across the neck region.

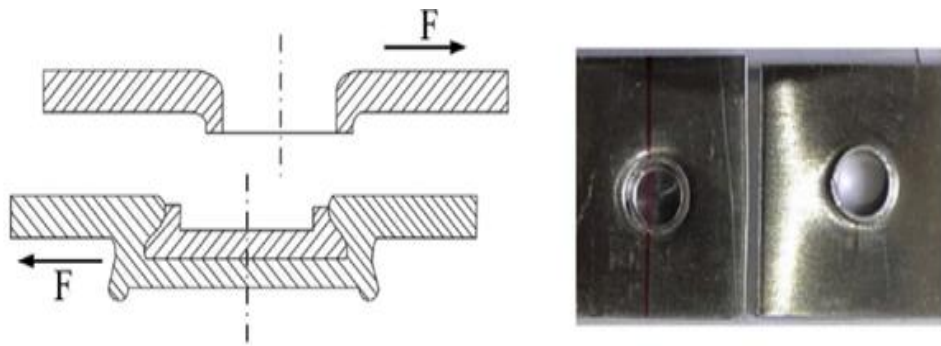


Figure 13 Neck fracture mode of the clinched joint [8]

(b) Hybrid neck fracture- Button failure in clinching typically refers to a specific type of failure mode that can occur during the clinching process, particularly when joining materials using protrusion-style clinching joints.

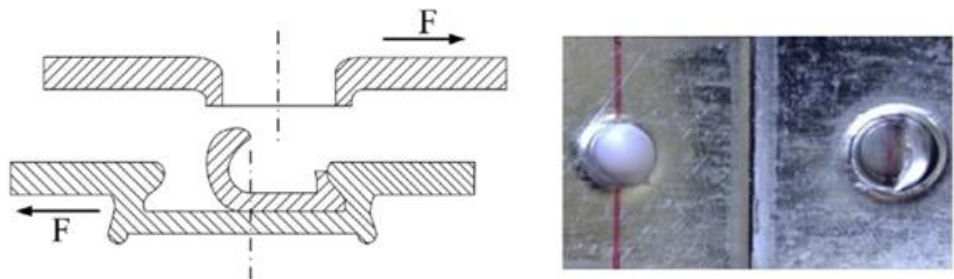


Figure 15 Hybrid neck fracture mode of the clinched joint [8]

(c) Hybrid button separation - This failure involves partial tearing around the interlock (button) region along with some interface separation. It shows that the joint failed partly due to mechanical interlock weakening and partly due to material separation under load. It's often seen when the interlock is not deep or strong enough.

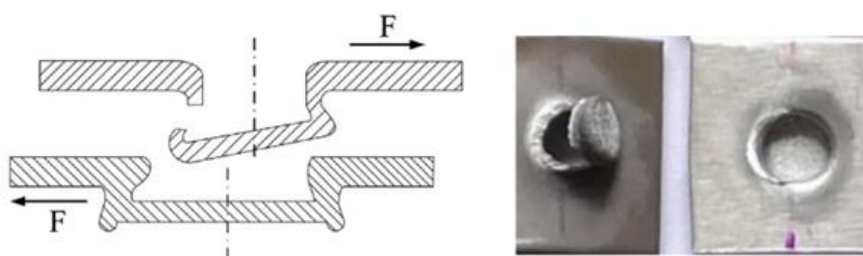


Figure 15 Hybrid button separation mode of the clinched joint [8]

(d) Button Separation - In this case, the joint fails completely at the interface where the two sheets are interlocked. The clinched button pulls out cleanly without tearing the sheet material significantly. This type of failure typically occurs when the interlock is shallow or not well-formed, making the joint prone to separation under load.

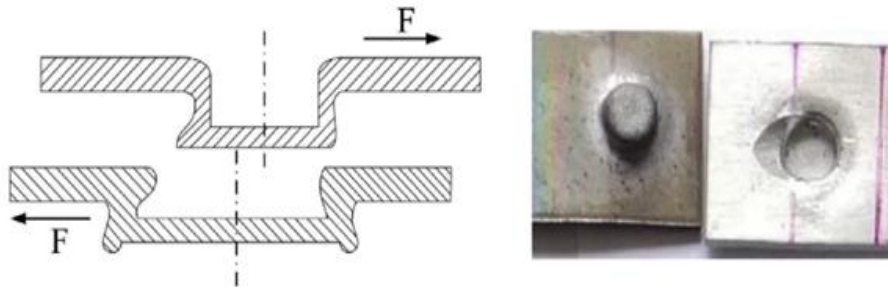


Figure 16 Button separation mode of the clinched joint [8]

2.14 Joining of galvanized mild steel to 5083 aluminum alloy using a combined clinching and resistance spot welding process

Ren, Dixin, et al [9] investigated novel hybrid joining technique that combines mechanical clinching with resistance spot welding (RSW) to effectively join galvanized mild steel and 5083 aluminum alloy sheets, both 1 mm thick. This method addresses the challenges of joining dissimilar materials, particularly the formation of brittle intermetallic compounds (IMCs) at the interface. The clinching process mechanically interlocks the sheets, while RSW provides localized heat to form a weld nugget, enhancing joint strength. Their study utilized punch-die electrodes and employed numerical simulations to analyze stress distribution and tensile shear strength under varying welding parameters. The findings showed that the hybrid method can reach a maximum failure load of around 4.5 kN, with a broad range of settings producing strong joints. It was observed that the interplay between welding current and welding time greatly affects joint strength, emphasizing the need to carefully optimize these factors to ensure consistent and dependable welds. This novel technique presents a valuable option for the automotive sector, where creating lightweight yet durable multi-material joints is critical.

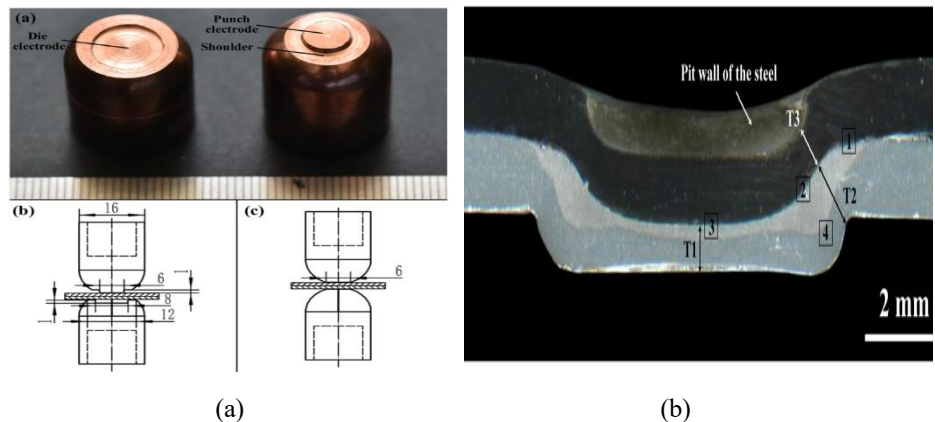


Figure 17 (a) Resistance punch and die electrode (b) Cross-section of clinch-resistance spot welding (CRSW) joint [9]

2.15 Joining of aluminum alloy and mild steel sheets using mechanical clinching.

Y. Abe et al. [10] performed an in-depth study on joining aluminum alloy and mild steel sheets through mechanical clinching, a technique that creates a mechanical interlock by deforming the materials without using rivets, welding, or adhesives. Their research combined experimental testing and finite element analysis to thoroughly investigate material deformation during clinching and to detect possible problems like cracks or incomplete joints. A major conclusion from their work was that the thickness of the sheets significantly influences the quality of the joint. If the upper sheet is too thin compared to the total stack thickness, it is prone to fracture; if the lower sheet is too thin, it may neck or separate, compromising joint strength. They also discovered that the material configuration affects the joining range placing the aluminum alloy on top of the steel sheet produced better results than the reverse setup. This is due to differences in how each material responds to force: aluminum is softer and deforms more easily, while steel has higher flow stress, making the interlocking more effective when the softer aluminum is on top. Overall, their findings help improve the understanding of mechanical clinching, especially in multi-material applications like automotive manufacturing, where strong, reliable joints between dissimilar materials are essential for both structural integrity and weight reduction.

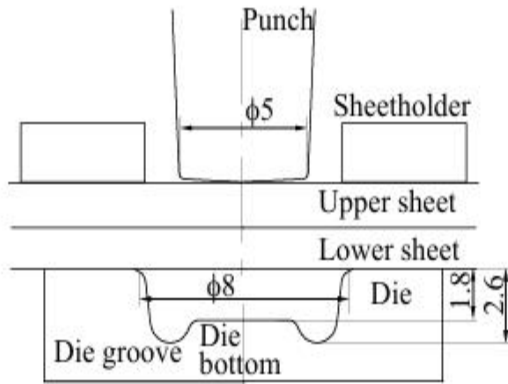


Figure 18 Deformation behavior of sheets in clinching [10]

2.16 Simulation analysis of the clinching process

Pritam Kamble et al [11] conducted a study on parametric Study of Clinched Joint," explores the clinching process, a method used to join sheet metals without fasteners, which is particularly valuable in industries like automotive manufacturing. The research focuses on the challenges of joining dissimilar materials, especially aluminum, which is known for its lightweight, high strength, and corrosion resistance. Using LS-DYNA software, the research models the clinching process and examines variables such as die groove diameter, punch corner radius, and punch stroke to assess their effects on joint performance. The findings indicate that increasing the punch stroke enhances joint strength, while modifying die diameters and punch corner radii helps improve material thickness and minimize defects. The study also recommends ideal setups for clinching, such as positioning the stronger material on the punch side and the thicker sheet on the die side. These conclusions offer important guidance for optimizing clinching to achieve stronger, more dependable joints in lightweight materials commonly used in automotive manufacturing.

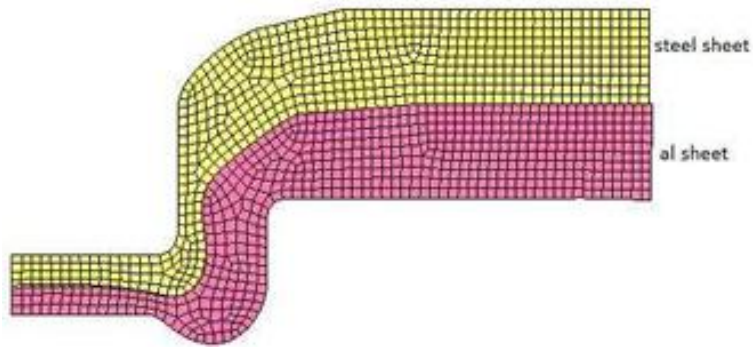


Figure 19 Axis symmetric 2d setup of clinched joint of dissimilar sheet [11]

2.17 Conclusion from literature survey

Clinching and resistance spot welding are two important methods used to join metal sheets, especially in industries like automotive manufacturing where using different materials and keeping things lightweight is essential. Resistance spot welding is effective for joining strong, conductive metals and produces fast, robust joints, but it requires careful control to prevent issues such as weak welds or metal splashing. Conversely, clinching connects materials without applying heat, rivets, or adhesives, making it an ideal method for joining metals like aluminum and steel that are difficult to weld using conventional techniques. Still, clinching needs the right sheet thickness and tool shape to make sure the joint holds properly and doesn't break apart. Each method has its own strengths and limits, and in some cases, using both together can lead to better, more dependable results. To get the best outcome, it's important to understand how these processes work and how to adjust them for different materials and designs.

Chapter 3

Methodology

3.1 Experimental procedure for three-sheet resistance spot welding process

In resistance spot welding, metal sheets are joined through a fusion welding technique by applying pressure and passing an electric current through the contact point using specially designed electrodes. The electrical resistance at the interface generates heat, causing the metal to melt and form a weld nugget. As the current stops and the material cools, the molten metal solidifies to create a strong joint. This process does not require any additional fasteners or filler materials. The setup of the spot-welding machine is illustrated in Figure 20.



Figure 20 Schematic setup of the RSW machine (a) Complete setup of the machine(b) Enlarged view of the working zone, and (c) Air compressor used in the welding process

In this experiment, stainless steel 304 (SS), mild steel 1006 (MS), and galvanized iron (GI) sheets, each 0.8 mm thick (measuring 30 mm × 100 mm), were used for spot welding. The sheets were first cleaned with acetone to remove dust and surface rust, and a 30 mm overlap area was marked to guide the welding process. Spot welding was performed using pointed electrodes while varying the pressure to identify the optimal setting, with the squeeze time, weld time, and hold time kept constant. Once the best pressure was determined, weld time was further optimized due to its significant impact on weld quality. The optimal parameters were found to be 4 bar pressure and 700

milliseconds weld time.

Following parameter optimization, experiments were conducted to study different stacking sequences of the three sheets. Among the configurations tested, the arrangement with stainless steel on top, mild steel in the middle, and galvanized iron at the bottom produced the most durable and strongest weld joints.

To better understand the weld nugget formation and behavior during spot welding, a numerical simulation was performed using LS-DYNA on a three-layer stack consisting of SS304, MS1006, and GI. This simulation enabled examination of temperature profiles, material deformation, and thermal-mechanical effects throughout the welding cycle.

To evaluate the mechanical strength of the welds, lap shear and peel tests were conducted using a universal testing machine (UTM). The lap shear test, carried out at a speed of 1 mm/min, assessed the load capacity of the joints and identified failure modes under shear loading. In the peel test, the top and bottom sheets were bent to a 90° angle, and testing at the same speed measured bonding effectiveness and resistance to peeling forces. Additional investigations were done to explore the internal joint structure. Microstructural examinations at 20x, 50x, and 100x magnifications helped analyze the weld nugget and the deformation in adjacent material. Scanning Electron Microscopy (SEM) provided high-resolution images of the weld zone, detecting defects such as cracks or porosity. This evaluation gave valuable information about the weld quality and dependability across various sheet stacking configurations. Furthermore, Energy Dispersive Spectroscopy (EDS) was employed to analyze the elemental makeup at the weld interface in the three-sheet stack. EDS mapping illustrated the distribution of important elements including iron (Fe), carbon (C), chromium (Cr), and nickel (Ni) within the weld area.

The mechanical characteristics of the stainless, mild and galvanized steel materials employed in the spot welding joints production, as well as in the clinching joint production, are detailed in Table 1. The mechanical properties of the copper electrode used in the RSW process are also listed in Table 1.

Table 1 Mechanical properties of the materials used in the three-sheet experiment

| Metal sheet | Density (g/cm ³) | Yield strength (MPa) | Tensile strength (MPa) | Young's modulus (GPa) | Poisson's Ratio |
|------------------|------------------------------|----------------------|------------------------|-----------------------|-----------------|
| SS 304 | 7.85 | 248 | 505–735 | 193 | 0.29 |
| GI | 7.85 | 200–550 | 270–550 | 200 | 0.29 |
| MS 1006 | 7.8 | 215 | 370–440 | 210 | 0.29 |
| Copper electrode | 8.9 | 110–130 | 70–110 | 200–400 | 0.34 |

Figure 21 (a) presents the dimensions of the samples SS 304 on top, MS 1006 in the middle, and GI at the bottom and Figure 21 (b) presents a schematic diagram of the spot-welding process used to join three sheets using optimized parameters of 4 bar pressure and a weld time of 700 milliseconds.

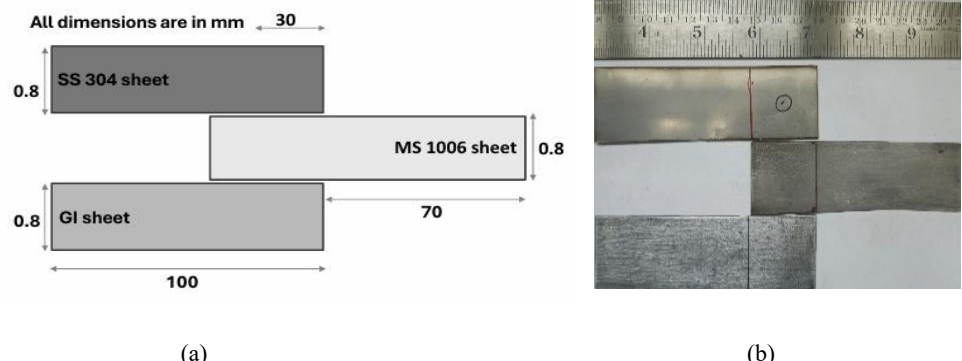


Figure 21 Dimension of samples (a) before spot welding, (b) after spot welding.

3.2 Experimental procedure for two-sheet spot welding and clinching process

In clinching, metal sheets are joined through a cold-forming technique where pressure is applied using specially shaped tools to deform the materials and create a mechanical lock between them. This process does not need any extra components like rivets or adhesives. The machine setup used for this process is shown in the figure 22.

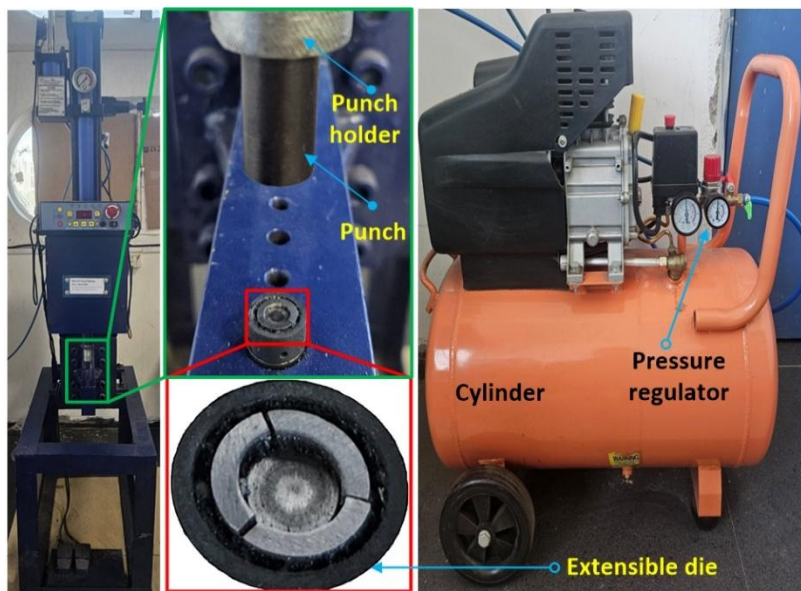


Figure 22 Schematic setup of the clinching machine (a) Complete setup of the machine(b) Enlarged view of the working zone, and (c) Air compressor used in the clinching process

In this study, 0.8 mm-thick mild steel sheets (measuring 30 mm × 100 mm) were cleaned with acetone and marked with a 30 mm overlap area for joining. The sheets were joined using two different techniques, spot welding and mechanical clinching, both separately and in combination, using two different sequences. Spot welding was performed using pointed electrodes with diameters of 6 mm (upper) and 16mm (lower), under varying pressures to determine the best welding conditions, followed by optimization of weld time. Clinching was done using a three-movable extensible die setup at different pressure levels to identify suitable forming conditions. For combined joining, two sequences were tested (1) spot welding followed by clinching using a pointed electrode, and (2) clinching followed by spot welding, where the initial clinching was performed using a

three-movable extensible die setup, followed by spot welding using punch-die-shaped electrodes with 1 mm diameter for both the upper and lower tools. A numerical simulation was also performed using LS-DYNA software to gain deeper insights into the behavior of the weld nugget during spot welding and to analyze the material flow characteristics in the clinching process.

To assess the strength and performance of the joints, lap shear and peel tests were conducted using a universal testing machine (UTM). For the lap shear test, parameters included a test speed of 1 mm/min, a gauge length of 30 mm, and a sheet thickness of 0.16 mm. The peel test was used to study joint strength, failure modes, and energy absorption. During the test, specimens were bent to 90 degrees & mounted in the UTM jaws, and load was applied until failure. The resulting fracture load was plotted against displacement to analyse joint performance.

The results showed that spot welding followed by clinching produced stronger and more reliable joints. In contrast, starting with clinching caused alignment issues that reduced weld quality. To better understand the properties of the joint, microstructural analysis and SEM were used to observe how the material flowed and how the weld was formed. XRD and EDS results showed a high presence of iron (Fe) and a small amount of carbon (C), which is typical for mild steel. EDS mapping helped visualize how iron was distributed across the welded area. The Fe K α 1 map revealed that iron was spread evenly throughout the joint, indicating good bonding between the materials during the clinching and welding process. This uniform distribution is crucial for ensuring the strength and overall quality of the joint.

The mechanical properties of the mild steel materials used in the RSW joint production, as well as in the clinched joint production, are listed in Table 2. The mechanical properties of the copper electrode used in the RSW process are also listed in Table 2.

Table 2 Mechanical properties of the materials used in the two-sheet experiment

| Metal sheet | Density (g/cm ³) | Yield strength (MPa) | Tensile strength (MPa) | Young's modulus (GPa) | Poisson's Ratio |
|------------------|------------------------------|----------------------|------------------------|-----------------------|-----------------|
| MS 1006 | 7.8 | 215 | 370-440 | 210 | 0.29 |
| Copper electrode | 8.9 | 110-130 | 70-110 | 200-400 | 0.34 |

The dimensions of the sample of the mild steel used in the experiments are shown in 23. The overlap length maintained in the study is 30 mm. Two different types of electrodes were used in the RSW process, and the same is shown in figure 24 (a) and figure 25 (b).

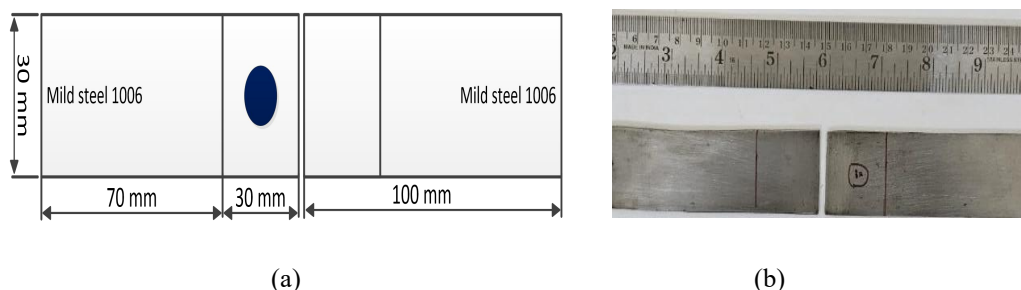
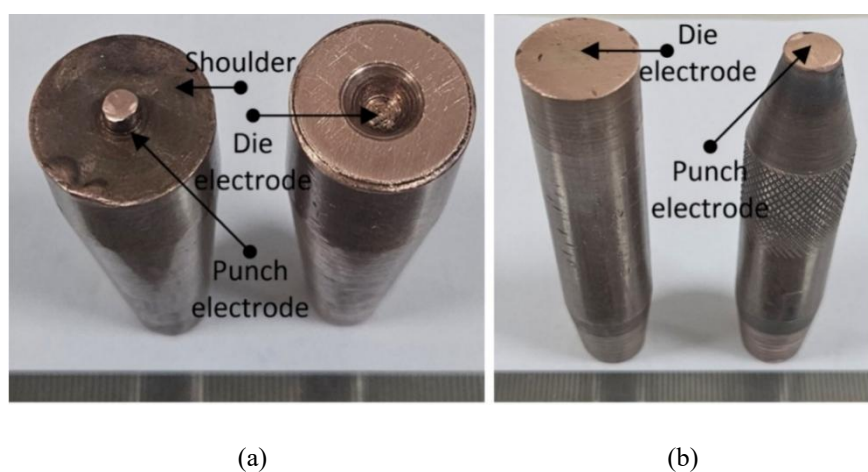


Figure 23 Dimensions of the sample prepared for mechanical clinching



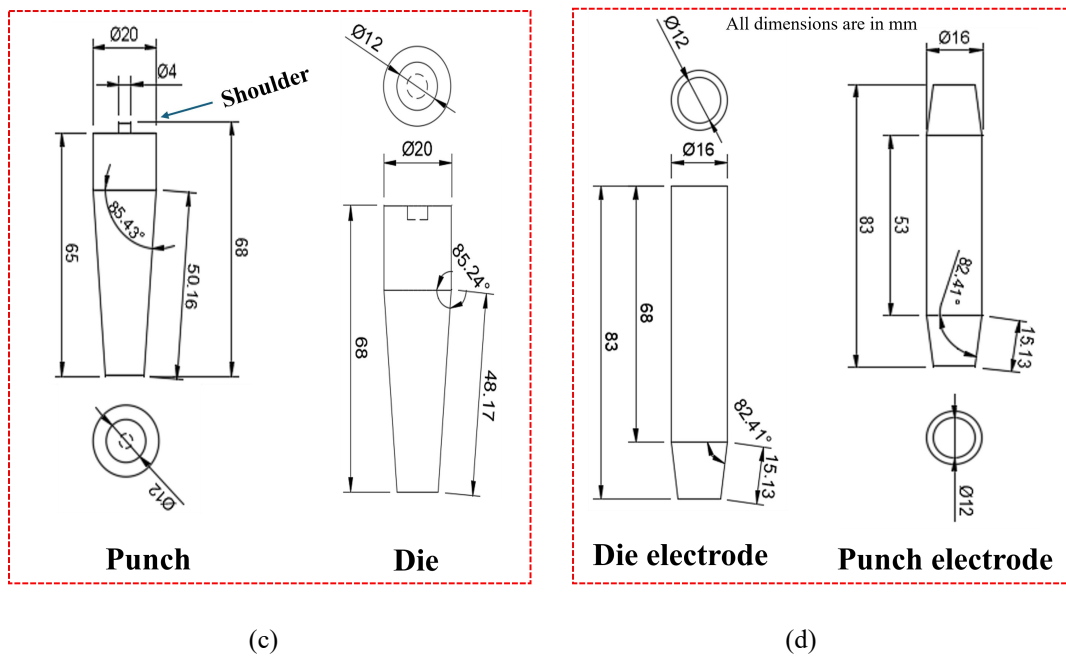


Figure 24 Two different types of electrodes used (a) punch and die type actual (b) pointed type actual (c) punch and die dimension (d) pointed type dimension.

3.3 Mechanical testing and characterization instruments

(a) Shearing machine - Shearing machine is a tool used to cut or trim large sheets of material, such as metal into smaller more manageable pieces. It works by applying a high amount of force to the material, essentially "shearing" it like a pair of giant scissors. The samples for the experiment were cut into 30 x 100 mm pieces using a shearing machine.

(b) Bench Grinder - A bench grinder is a power tool that is commonly used in workshops and manufacturing areas for grinding, sharpening, shaping, and polishing metal or other hard materials. It consists of a motor mounted on a bench with two grinding wheels attached on either side. The cut samples (30 mm x 100 mm) were finished using a bench grinder.

(c) Lathe machine - A lathe machine is used to shape or cut materials like metal by rotating the material against a cutting tool. It spins the material while a tool shaves off pieces, creating shapes like cylinders or cones. The main tasks of a lathe include turning, facing, and drilling. It's commonly used to make cylindrical

parts like shafts, rods, and bushings. Punch-die type and pointed type copper electrodes for resistance spot welding were fabricated using a turning operation.

(d) UTM machine - A Universal Testing Machine (UTM) is used to test the strength of materials. It can apply tension, compression, or bending forces to a sample and measures how much the material stretches or breaks. This helps in understanding the material's mechanical properties like strength and flexibility.

(e) Double Disc polishing machine - A double disc polishing machine is used to smooth the sample's surface and remove scratches using polishing papers on two rotating discs. Papers of grit sizes 320, 600, 800, 1000, 1200, 1500, 2000, and 2500 are used, followed by diamond paper with diamond paste of 0.5-0.1micron were used for fine polishing. This prepares the sample for clear viewing under a microscope.

(f) Digital microscope - A digital microscope is a type of microscope that uses digital technology to capture high-quality images of very small details inside materials. When studying microstructure, it helps us see tiny features, such grains, cracks, and layers, in materials that we can't see with the naked eye.

(g) Optical Microscope - An optical microscope helps us see tiny details in materials that we can't see with our eyes alone. It uses visible light and lenses to magnify the surface of a polished sample. We Used it to observe microstructure at 5x, 10x, 20x, 50x and 100x magnification.

Chapter 4

Results and Discussions

4.1 Simulation study of three-sheet resistance spot welding.

The RSW process involving three dissimilar metal sheets SS304, MS1006 and GI sheets was modeled using a two-dimensional setup in LS-DYNA. Each sheet had a thickness of 0.8 mm and was positioned between an upper copper electrode and a bottom electrode connected to ground. To accurately resolve the thermal profile and nugget development, a refined mesh ranging from 0.1 mm to 0.2 mm was applied in the weld region. The steel sheets were assigned appropriate temperature-dependent thermal and electrical characteristics, whereas the copper electrodes were treated as rigid conductors with excellent conductivity properties. Interface contact resistance was specified at the junctions between each layer and at the electrode-sheet interfaces to replicate the localized heating due to electrical resistance (Joule heating). Electrical potential was introduced at the upper electrode, while the bottom electrode acted as a ground, ensuring current flow through the multilayer stack. All relevant heat transfer mechanisms—conduction, convection, and radiation—were included to enhance thermal modeling accuracy. The simulation employed an implicit thermal solver for stable and reliable temperature field calculations, with time control parameters fine-tuned for consistent and efficient convergence.

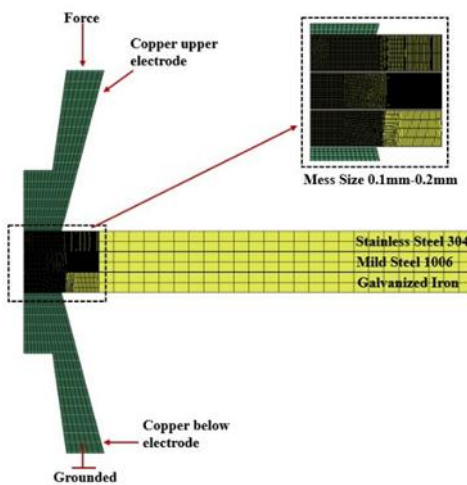


Figure 25 Axis symmetric 2d simulation setup for spot welding of three sheets

4.2 Simulation study of two-sheet resistance spot welding.

The electrode and sheet arrangement in the finite element model (FEM) is shown in Figure 26. A two-dimensional LS-DYNA model was used to simulate the resistance spot welding (RSW) process for joining two mild steel sheets, each 0.8 mm thick, placed between a top copper electrode and a grounded bottom electrode. A fine mesh (0.1–0.2 mm) was applied in the weld zone to capture precise temperature gradients. The mild steel sheets were assigned thermal-electrical properties, while the electrodes were modeled as rigid bodies with high electrical conductivity. Electrical resistance was defined at the interfaces between sheets and electrodes to simulate Joule heating, which is critical for weld nugget formation. Voltage was applied to the upper electrode, with grounding at the lower electrode to complete the current path. Heat transfer through conduction, convection, and radiation was considered to enhance the accuracy of thermal behavior. An implicit thermal solver was used for better stability in the simulation, with time step settings adjusted for efficient convergence.

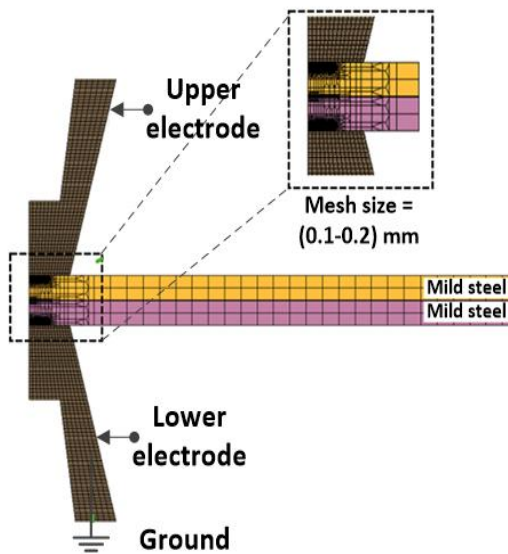


Figure 26 Axis symmetric 2d simulation setup for spot welding of two sheets

4.3 Simulation study of two-sheet mechanical clinching.

The tool and sheet arrangement in the finite element model (FEM) is depicted in Figure 27. A two-dimensional finite element model is employed for the clinching simulation using the explicit solver LS-DYNA software. All components involved in the simulation are discretized into four-noded quadrilateral elements. The punch, sliding sector, and extensible die are modeled as rigid bodies. At the same time, the upper and lower sheets are treated as deformable components, following the MAT 024 piecewise linear plasticity material model. The dimensions of the parts used in the numerical analysis are consistent with those of the experimental setup, with a 0.5 mm fillet radius applied to the punch, sliding sector, and die.

The sliding sector undergoes displacement in the x-direction, while the punch moves downward along with the negative y-direction. The adaptive meshing technique employed ensures optimal mesh quality throughout the analysis. The technique adjusts dynamically to control element distortion during deformation. Static Coulomb friction (coefficient 0.20) is applied between all contact pairs, including punch–upper sheet, upper–lower sheets, lower sheet–die, upper sheet–blank holder, and sliding sector–upper sheet. A 2D automatic surface-to-surface contact model defines interactions between the punch, sheet, sliding sector, and die. Displacement-time data is used as input, with the blank holder applying a load to hold the sheet in place.

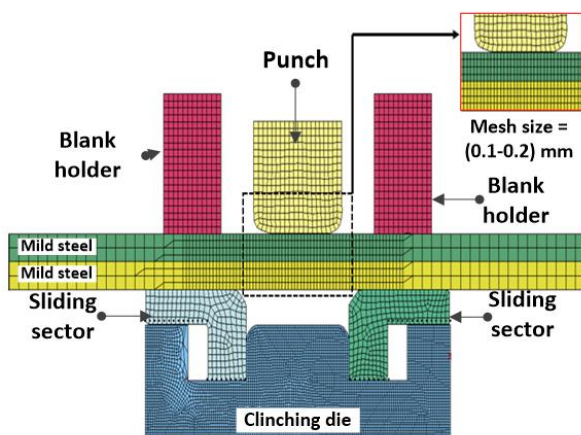


Figure 27 Axis symmetric 2d simulation setup for clinching of two sheets

Chapter 5

Results and Discussion

5.1 Joining of three dissimilar (SS 304, MS 1006, and GI) sheets of thickness 0.8 mm using resistance spot welding

Resistance spot welding (RSW) is commonly used to join three dissimilar metal sheets SS 304, MS 1006, and GI without filler material, using heat from electrical resistance and pressure. Each material contributes unique properties: SS 304 offers corrosion resistance, MS 1006 provides good formability, and GI adds zinc coating protection. RSW produces strong joints with minimal thermal distortion, making it ideal for multi-material assemblies.

A lap shear test was performed on a 0.24 mm-thick SS 304–MS 1006–GI joint using a 10 kN Universal Testing Machine. The specimen had a gauge length of 110 mm, with 30 mm gripped at each end, and testing was done at 1 mm/min crosshead speed. Figure 41 shows the specimen used for the lap shear and peel tests.

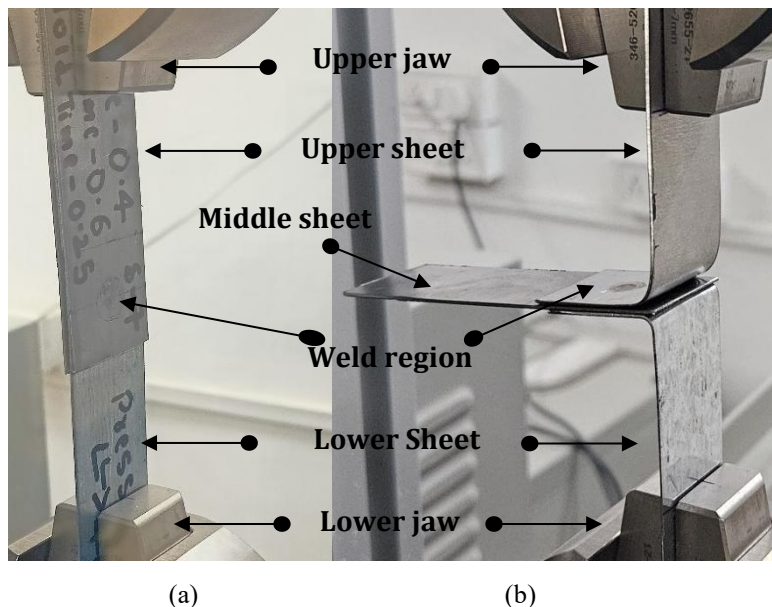


Figure 27 Arrangement made for 3 sheet mechanical tests (a)
Lap-shear test (b) Peel test

5.1.1 Effect of pressure on lap shear test

Three different pressure values (3, 4, and 5 bar) were used to prepare the joints using resistance spot welding. The squeeze time, weld time, and hold time were kept constant at 400 ms, 700 ms, and 250 ms, respectively. The results obtained from the tensile test were summarized in Table 3.

Table 3 Optimization of pressure parameters for three-sheet spot welding

| S.no | Squeeze time (Milliseconds) | Pressure (bar) | Weld Time (Milliseconds) | Hold time (Milliseconds) | Max Tensile Strength (N) |
|------|-----------------------------|----------------|--------------------------|--------------------------|--------------------------|
| 1 | 400 | 3 | 700 | 250 | 6237 |
| 2 | 400 | 4 | 700 | 250 | 7226 |
| 3 | 400 | 5 | 700 | 250 | 6748 |

Figure 28 (a) shows the failed sample after lap shear test. Figure 28 (b) illustrate the highest weld strength of 7226 N was achieved at 4 bar pressure as compared to 3 and 5 bar because it provided the right balance for a strong bond. At 3 bar, the pressure wasn't enough to properly join the metal sheets, resulting in a weaker weld whereas at 5 bar, although the strength was better than at 3 bar, but excessive pressure may have pushed out too much molten metal or made the joint too thin, reducing its strength. So, 4 bar pressure turned out to be the optimal pressure for getting the strongest and most reliable weld for three dissimilar sheets.

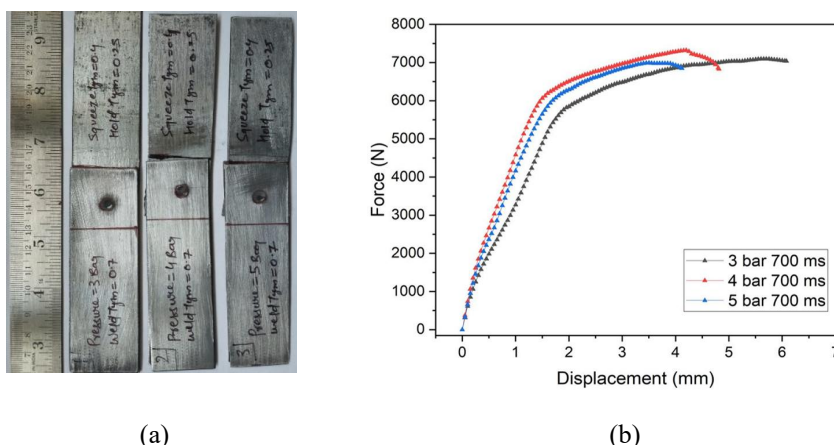


Figure 28 (a) Failed sample after lap shear test, (b) Results of the Lap shear test for various pressures

5.1.2 Effect of welding time on lap shear test

The weld time was varied while keeping the welding pressure constant at 4 bars. The squeeze time and hold time were fixed at 400 ms and 250 ms, respectively. The different weld times and the corresponding tensile strengths are shown in Table 4. The failed sample after the lap shear test is shown in Figure 29 (a)

Table 4 Optimization of weld time parameters for three-sheet spot welding

| S.no | Squeeze (Milliseconds) | Pressure (bar) | Weld Time (Milliseconds) | Hold time (Milliseconds) | Max Tensile Strength (N) |
|------|---------------------------|-------------------|-----------------------------|-----------------------------|-----------------------------|
| 1 | 400 | 4 | 300 | 250 | 5762 |
| 2 | 400 | 4 | 400 | 250 | 6574 |
| 3 | 400 | 4 | 500 | 250 | 6938 |
| 4 | 400 | 4 | 600 | 250 | 6815 |
| 5 | 400 | 4 | 700 | 250 | 7451 |
| 6 | 400 | 4 | 800 | 250 | 6711 |
| 7 | 400 | 4 | 900 | 250 | 6673 |
| 8 | 400 | 4 | 1000 | 250 | 6696 |

The highest strength of the joint obtained from the experiments was 7451 N at a 700 ms weld time as shown in Figure 29 (b). The higher strength of the joint at 700 ms is due to the right amount of heat and bonding. If the weld below the 700 ms strength of the joint was reduced due to not providing enough heat for the bonding, by varying the weld time. On the other hand, longer times like 800–

1000 ms slightly reduced the strength, probably because too much heat caused issues like metal expulsion or weakening of the weld area. So, 700 ms turned out to be the most effective weld time for getting a strong and reliable joint.

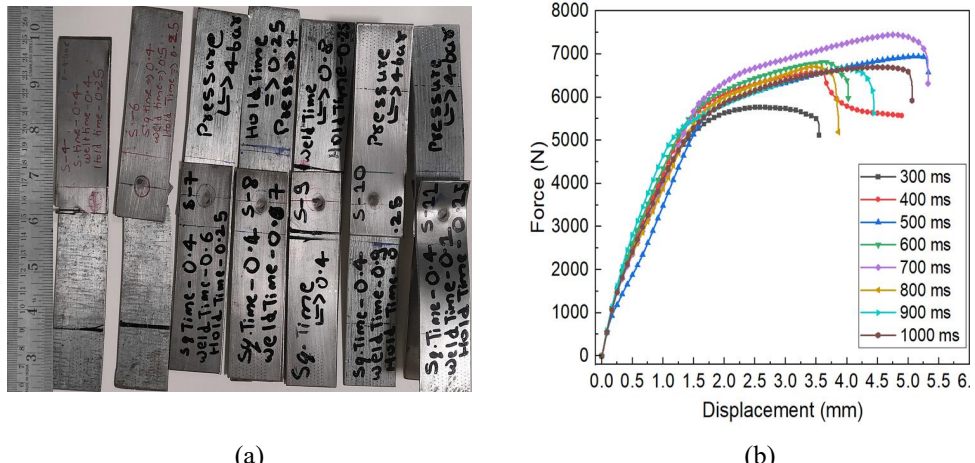


Figure 29 (a) Failed sample after lap shear test, (b) Results of the Lap shear test for various weld time

5.1.3 Effect of various combinations of three sheets on lap shear test

Experiments were performed at various combinations of three dissimilar sheets, keeping the variables constant, like pressure, weld time, squeeze time, and hold time at 4 bar, 700 ms, 400 ms, and 250 ms, respectively. The optimized results are summarized in Table 5. The failed sample after the lap shear test is shown in Figure 30 (a).

Table 5 Optimization of different material sheet combinations for three-sheet spot welding

| Metal Sheet | Squeeze time (Milliseconds) | Pressure (bar) | Weld Time (Milliseconds) | Hold time (Milliseconds) | Maximum Tensile Strength (N) |
|--------------------------------|-----------------------------|----------------|--------------------------|--------------------------|------------------------------|
| SS Top / MS Middle / GI Bottom | 400 | 4 | 700 | 250 | 11776 |
| SS Top / GI Middle / MS Bottom | 400 | 4 | 700 | 250 | 8878 |
| GI Top / MS Middle / SS Bottom | 400 | 4 | 700 | 250 | 7388 |
| GI Top / SS Middle / MS Bottom | 400 | 4 | 700 | 250 | 9089 |
| MS Top / SS Middle / GI Bottom | 400 | 4 | 700 | 250 | 8426 |

The highest strength, 11.776 kN, was obtained from the combination of SS on top, MS in the middle, and GI at the bottom, as shown in Figure30 (b). The above combination was given higher strength due to good ductility, likely because heat flowed well from stainless steel to mild steel, and having GI at the bottom avoided zinc issues. The SS–GI–MS setup showed moderate strength (8.9 kN), but zinc in the middle GI layer likely caused early failure. The GI–MS–SS combination had the lowest strength (7.4 kN) and failed early, probably due to zinc on the top GI sheet vaporizing and weakening the weld. The GI–SS–MS layout showed decent strength (9.1 kN), but placing GI on top still caused some zinc-related issues. Lastly, the MS–SS–GI setup had moderate strength (8.4 kN) having GI at the bottom helped, but MS on top limited heat, resulting in a weaker weld.

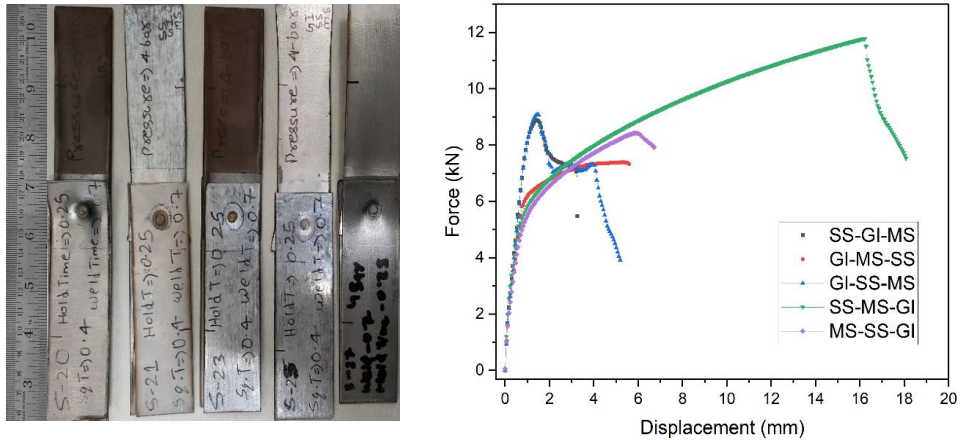


Figure 30 (a) Failed sample after lap shear test (b) Results of the Lap shear test for various three sheet-combination

5.1.4 Peel test

A peel test was conducted to evaluate the weld strength of a multi-material stack-up comprising SS 304 on the top, MS 1006 in the middle, and galvanized iron (GI) at the bottom. The MS sheet was kept free during testing, while the SS and GI sheets were clamped using L-shaped fixtures and held firmly between the jaws of a Universal Testing Machine (UTM). This setup applied a peeling force perpendicular to the weld interface. The welding pressure, squeeze time, weld time, and hold time were kept constant at 4 bar, 400ms, 700ms, and 250ms, respectively. The failed sample after the lap shear test is shown in Figure 31 (a). The results are summarized in Table 6.

Table 6: Peel test results for three-sheet spot welding

| Metal sheet | Squeeze time (Milliseconds) | Pressure (bar) | Weld Time (Milliseconds) | Hold time (Milliseconds) | Max Tensile Strength (N) |
|---------------------------------|-----------------------------|----------------|--------------------------|--------------------------|--------------------------|
| SS Top / MS middle / GI Bottom. | 400 | 4 | 700 | 250 | 234 |

The peel test results indicate that higher strength was obtained in the combination of SS 304 on the top, MS 1006 in the middle, and galvanized iron (GI) at the bottom. The values are 234 N as shown in Figure 31 (b). For the above combination lap shear test given high strength compared to peel test results because all layers worked together and the weld was strong while peel test gave low strength because the bottom GI layer is weaker and more likely to fail under bending.

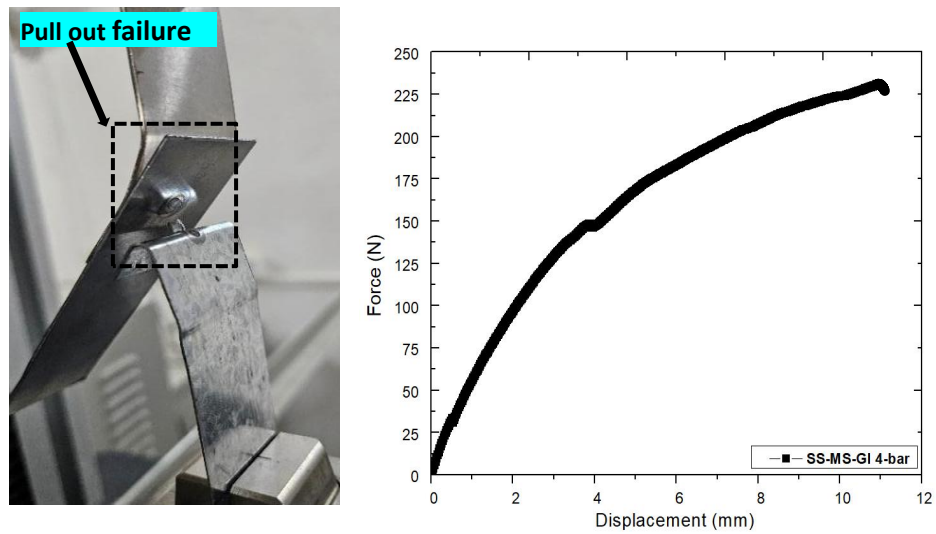


Figure 31 (a) Failed sample after peel test, (b) Results of the peel test

5.1.5 Cross-section analysis of weld nugget in three-dissimilar sheets spot welding

In RSW, the quality of the joint is heavily influenced by the formation and geometry of the weld nugget. When welding three dissimilar metal sheets, the position of each material in the stack affects heat distribution, current flow, and nugget growth. To understand which sheet arrangement yields the best weld, six different stacking combinations of SS304, galvanized iron (GI), and MS 1006 were experimentally tested.

The nugget geometry was analyzed based on two key parameters:

- Nugget Diameter (a) represents the width of the fused zone.
- Penetration Depth (b) indicates how deeply the weld has penetrated into the stack.

From the Figure 32, the configuration with SS on top, MS in the middle, and GI at

the bottom produced the largest nugget diameter (4.255 mm) and greatest penetration (1.555 mm), indicating the strongest and most complete fusion. Other configurations showed smaller nugget sizes and less penetration, suggesting weaker joints.

This variation occurs due to differences in electrical resistivity and thermal conductivity of the materials. For instance, SS generates more heat due to higher resistivity, while GI may lead to poor fusion if placed in high-resistance zones due to zinc coating evaporation. These observations help optimize sheet positioning for achieving maximum weld strength and quality in multi-layer spot welding applications.

Table 7 Nugget geometry for different stacks

| S.no | Metal Sheet | Nugget diameter | Penetration depth |
|-------------|--------------------------------|------------------------|--------------------------|
| 1 | SS Top / MS Middle / GI Bottom | a = 4.255 mm | b = 1.555 mm |
| 2 | SS Top / GI Middle / MS Bottom | a = 4.255mm | b = 1.555 mm |
| 3 | GI Top / MS Middle / SS Bottom | a = 4.255 mm | b = 1.555 mm |
| 4 | GI Top / SS Middle / MS Bottom | a = 4.255 mm | b = 1.555 mm |
| 5 | MS Top / SS Middle / GI Bottom | a = 4.255 mm | b = 1.555 mm |
| 6 | MS Top / GI Middle / SS Bottom | a = 4.255 mm | b = 1.555 mm |

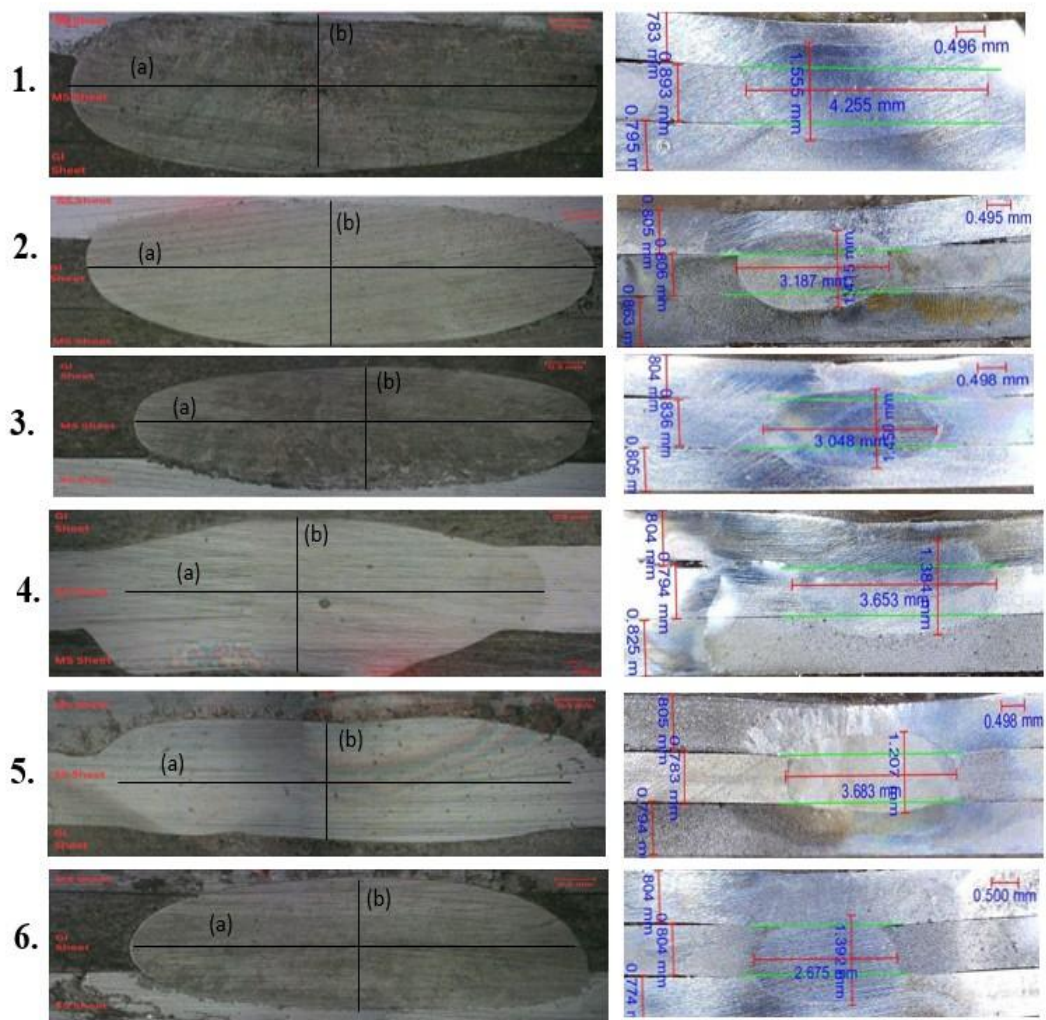


Figure 32 Weld nugget geometry analysis for various combinations of sheets

5.1.6 Energy dispersive spectroscopy analysis on three-sheet spot welding.

The Energy Dispersive Spectroscopy (EDS) was employed to analyse the elemental composition across the welded interface in the three-sheet stack, comprising a GI sheet on top, MS in the middle, and SS at the bottom. The EDS spectrum obtained from the weld region (Spectrum 8) shows the composition of various elements like iron (Fe) (88.1 wt%), Zinc (Zn) (6.0 wt%), chromium (Cr) (4.1 wt%), and nickel (Ni) (1.7 wt%) as shown in Figure 33 consistent with the ferrous nature of all three materials,

Minor peaks of zinc (Zn) (6.0 wt%) indicate the diffusion of the zinc coating from the GI sheet into the weld zone. This is expected due to the heat generated during

spot welding, which can cause partial melting or vaporization of the zinc coating, allowing it to migrate.

The presence of chromium (Cr) (4.1 wt%) and traces of nickel (Ni) (1.7 wt%) confirms the contribution of the stainless steel (SS304) bottom sheet to the weld nugget. SS304 typically contains 18–20% Cr and 8–10.5% Ni, and their diffusion into the weld zone is indicative of metallurgical bonding involving all three sheets.

Thus, Figure 33 (a) EDS data support successful material mixing during the spot-welding process and validate the formation of a joint involving GI, MS, and SS through diffusion of key alloying elements.

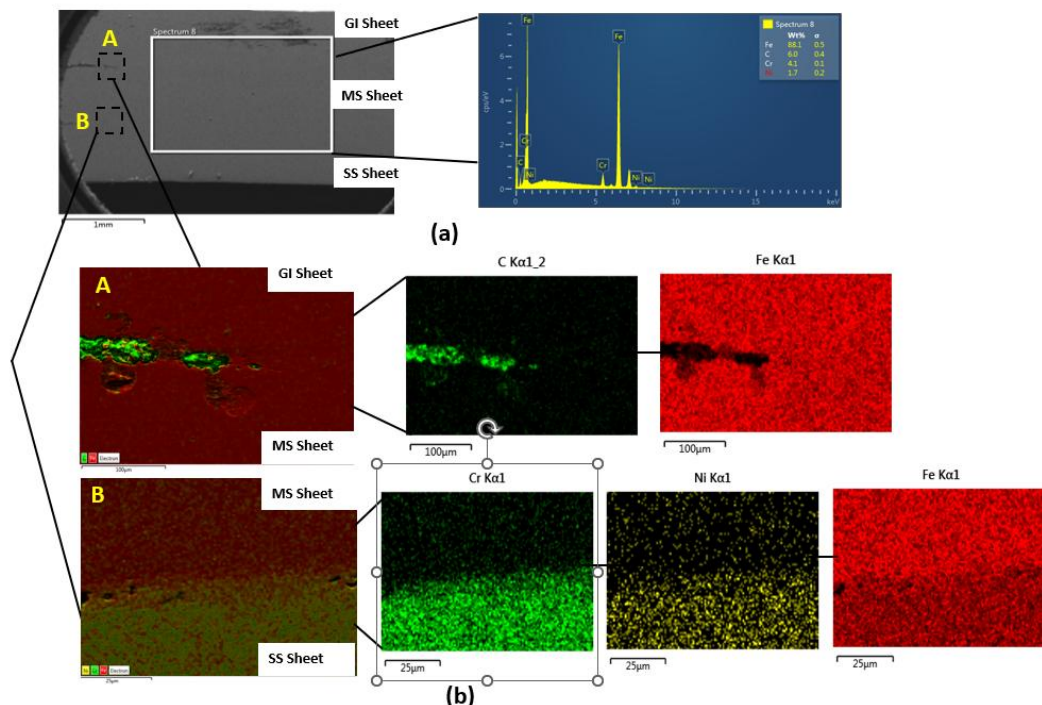


Figure 33 EDS analysis on (a) Area of three sheet spot welding (b) mapping of three sheet spot welding

Figure 33 (b) EDS mapping was also carried out to examine the distribution of key elements (Fe, C, Cr, Ni) across the welded region in the three-sheet spot welded stack consisting of GI (top), MS (middle), and SS (bottom) sheets. Each element's presence gives insight into the bonding behavior and elemental diffusion during the welding process. The findings are described below:

The **Fe K α 1 map** shows a uniform distribution of iron across all three sheets, confirming good metallurgical bonding among GI, MS, and SS sheets.

The **C K α 1 map shows** carbon is concentrated at the GI–MS interface, possibly due to surface contamination or heat-induced migration during welding.

The **Cr K α 1 map shows** chromium is clearly concentrated in the SS sheet, confirming its identity and indicating limited diffusion into other layers.

The **Ni K α 1 map shows** nickel is also confined to the SS region, showing stable composition with minimal intermixing.

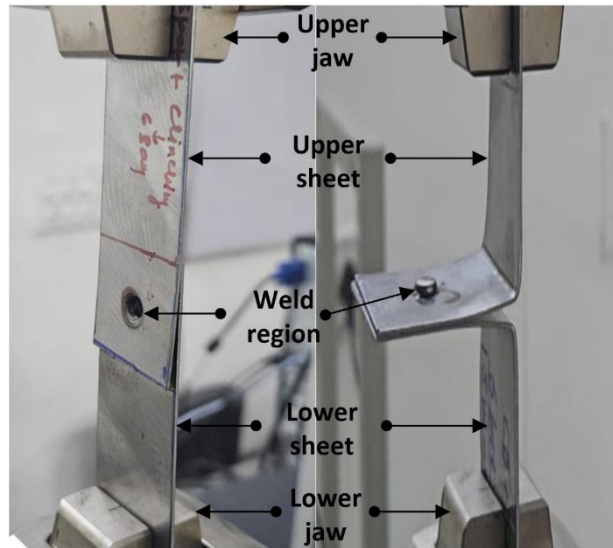
Zinc (Zn) Zinc was not detected, likely due to evaporation or loss during the welding process, which is typical in galvanized sheets.

5.2 Joining of two Mild steel (MS 1006) sheets of thickness 0.8 mm using resistance spot welding and clinching process

Joining two MS 1006 sheets, each having a thickness of 0.8 mm, using the RSW and clinching process is commonly used in sheet metal applications. RSW uses heat generated by electrical resistance along with applied pressure to form a strong, localized weld without the need for filler material. Mechanical clinching, on the other hand, is a cold joining process that mechanically locks the sheets through localized plastic deformation without melting.

MS 1006 is widely used in automotive and industrial applications due to its excellent formability, weldability, and cost-effectiveness. Comparing RSW and clinching allows for an evaluation of joint strength, structural integrity, and process suitability for thin sheet metal assemblies.

The lap shear test of a joint comprising 0.16 mm-thick sheets of MS 1006 was conducted using a Universal Testing Machine (UTM) with a 10 kN load capacity. A gauge length of 110 mm was maintained, with 30 mm held in the grips at both ends. The pull-out test was carried out at a crosshead speed of 1 mm/min. Figure 3 shows the specimen used for the lap shear test and peel test for three dissimilar sheets.



(a)

(b)

Figure 34 Arrangement made for 2 sheet mechanical tests (a)
Lap-shear test (b) Peel test

5.2.1 Effect of welding pressure on lap shear test.

Four different pressure values (3, 4, 5 and 6 bar) were used to prepare the joints using resistance spot welding. The squeeze time, weld time, and hold time were kept constant at 400 ms, 700 ms, and 250 ms, respectively. The corresponding maximum tensile strengths are listed in Table 8.

Table 8 Optimization of pressure parameters for two-sheets spot welding

| S.no | Pressure(bar) | Weld time (ms) | Squeeze time (ms) | Hold time (ms) | Peak load (N) |
|------|---------------|----------------|-------------------|----------------|---------------|
| 1 | 3 | 700 | 400 | 250 | 5309 |
| 2 | 4 | 700 | 400 | 250 | 6050 |
| 3 | 5 | 700 | 400 | 250 | 5561 |
| 4 | 6 | 700 | 400 | 250 | 5299 |

The highest weld strength of 6050 N was obtained at 4 bar pressure, as it offered the right balance between contact and heat generation. At 3 bar, the pressure was too low, leading to poor contact and uneven heating, which caused a lower

strength of 5309 N. When the pressure was increased to 5 bar, the strength slightly improved to 5561 N, but the excess pressure likely reduced electrical resistance, limiting heat generation and nugget size. At 6 bar, the strength dropped again to 5299 N, probably due to too much squeezing, which may have pushed out molten metal or thinned the weld zone. Hence, 4 bar proved to be the most effective pressure for achieving a strong and reliable weld.

As it is observed from the figure 35 (a) that failure mechanism of the joint was button failure and (b) maximum load carried by the joint was 6050 N.

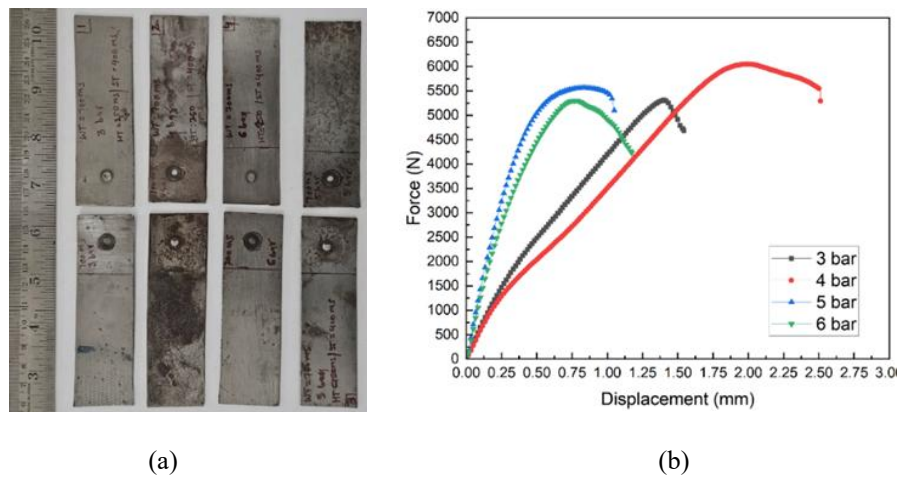


Figure 35 (a) Failed sample after lap shear test (b) Results of the lap shear test for various pressure.

5.2.2 Effect of welding time on lap shear test.

In the next set of experiments, the weld time was varied while keeping the welding pressure constant at 4 bar. The squeeze time and hold time were fixed at 400 ms and 250 ms respectively. The different weld times and the corresponding tensile strengths are shown in Table 9.

Table 9 Optimization of weld time parameters for two-sheets spot welding

| S.no | Pressure(bar) | Weld Time(ms) | Squeeze Time (ms) | Hold Time(ms) | Highest Strength (N) |
|------|---------------|---------------|-------------------|---------------|----------------------|
| 1 | 4 | 500 | 400 | 250 | 5360 |
| 2 | 4 | 600 | 400 | 250 | 5349 |
| 3 | 4 | 700 | 400 | 250 | 5343 |
| 4 | 4 | 800 | 400 | 250 | 5810 |
| 5 | 4 | 900 | 400 | 250 | 6072 |
| 6 | 4 | 1000 | 400 | 250 | 5372 |
| 7 | 4 | 1100 | 400 | 250 | 5210 |

The best weld strength of 6071 N was achieved at a weld time of 900 ms with 4 bar pressure. Shorter weld times like 500, 600, and 700 ms didn't give enough heat, so the metals didn't fuse properly, leading to lower strength. At 800 ms, the joint got stronger as more heat improved the fusion. The strongest weld formed at 900 ms, where the heat was just right to create a solid nugget without melting too much. But when the time went beyond 900 ms, the weld started to weaken again probably because too much heat caused metal to melt and escape or damaged the joint. So, 900 ms was the sweet spot for a strong, clean weld.

As it is observed from the figure 36 (a) that failure mechanism of the joint was button failure and (b) maximum load carried by the joint was 6050 N

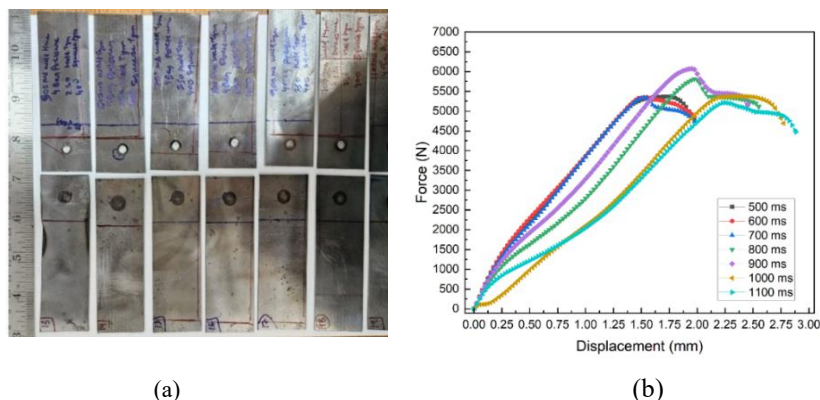


Figure 36 (a) Failed sample after lap shear test (b) Results of the lap shear test for various weld time

5.2.3 Effect of clinching pressure on lap-shear strength

In the next set of experiments, five different pressure values (4, 4.5, 5, 5.5, 6 bar) were used to prepare the clinching joints. The corresponding maximum tensile strengths are listed in Table 10.

Table 10 Optimization of pressure parameters for two-sheets mechanical clinching

| S.no | Pressure (bar) | Highest Strength (N) |
|------|----------------|----------------------|
| 1 | 4 | No Joint |
| 2 | 4.5 | 1821 |
| 3 | 5 | 1663 |
| 4 | 5.5 | 1749 |
| 5 | 6 | 2039 |

The highest joint strength of 2039 N in the mechanical clinching process was achieved at 6 bar pressure. At 4 bar, the pressure was too low to form a joint at all. With 4.5 bar, a joint was formed, but the interlock was weak, giving lower strength (1821 N). Slight improvements were seen at 5 and 5.5 bar (1663 N and 1749 N), but the interlocking wasn't strong enough, possibly due to poor material flow or small tears. At 6 bar, the pressure was just right—enough to allow good material flow and form a strong interlock without damaging the sheets. This made it the best condition for a strong, reliable joint.

As it is observed from the figure 37 (a) that failure mechanism of the joint was button failure and (b) maximum load carried by the joint was 2039 N.

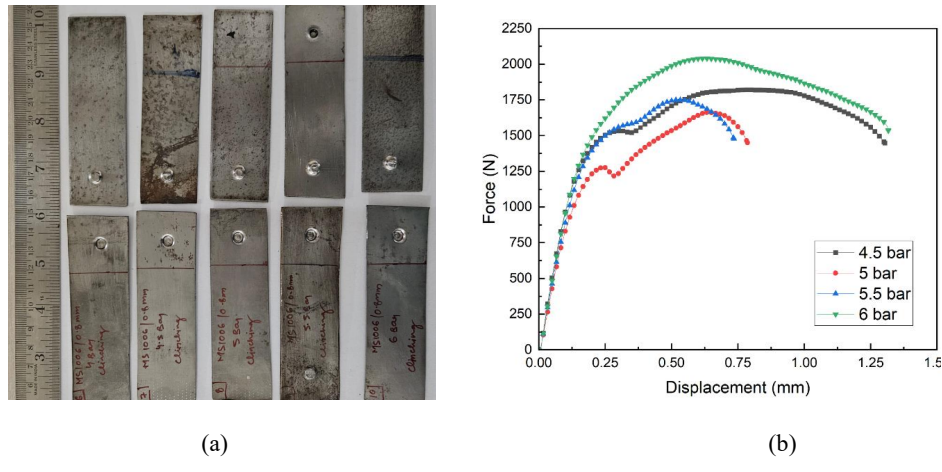


Figure 37 (a) Failed sample after lap shear test (b) Results of the lap shear test for various clinching pressure

5.2.4 Lap shear test

The lap test results for spot weld-assisted clinching and clinch-assisted spot welding are summarized in Tables 11 and 12, respectively. The optimized pressure used in the samples in the spot and clinching is 4 bar, 900 ms, and 6 bar, respectively. The Figure 38 shows that the highest lap shear strength, 6100 N, was achieved in the spot-welding assisted clinching, whereas 2015 N was achieved in the clinch assisted spot welding of the sheets. The results

Spot welding assisted clinching achieved higher strength because clinching gave a strong mechanical lock, and the spot weld added a solid metallurgical bond, together creating a much stronger joint.

Table 10 Lap shear test result for spot welding-assisted clinch joint

| S.no | Spot Pressure (bar) | Clinching Pressure (bar) | Weld Time (ms) | Squeeze Time (ms) | Hold Time (ms) | Peak Strength (ms) |
|------|---------------------|--------------------------|----------------|-------------------|----------------|--------------------|
| 1 | 4 | 6 | 900 | 400 | 250 | 6100 |

Table 11 Lap shear test result for clinch joint-assisted spot welding

| S.no | Clinching Pressure (bar) | Spot Pressure (bar) | Weld Time (ms) | Squeeze Time (ms) | Hold Time (ms) | Peak Strength (ms) |
|------|--------------------------|---------------------|----------------|-------------------|----------------|--------------------|
| 1 | 6 | 4 | 900 | 400 | 250 | 2015 |

As it is observed from the figure 38 (a) that failure mechanism of the joint was button failure and (c) maximum load carried by the joint was 6100 N.

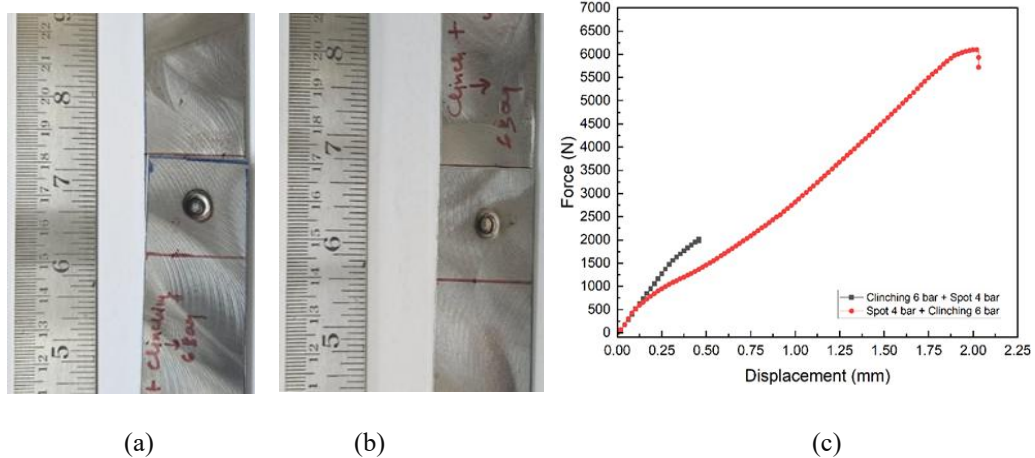


Figure 38 Failed sample after lap shear test (a) Spot welding assisted clinch joint (b) clinching assisted spot welding (c) Result of the lap shear test.

5.2.5 Peel test

The highest peel strength (2793 N) was achieved when clinching was done first at 6 bar, followed by spot welding at 4 bar. This sequence worked well because the strong clinch provided a solid mechanical lock, and the spot weld added extra bonding, making the joint more resistant to peeling. In comparison, doing spot welding first and then clinching gave lower strength (1736 N), likely because the heat from welding affected the material, weakening the clinch. So, spot welding after a proper clinch leads to a stronger, more durable joint.

Table 12 Peel test result for spot welding-assisted clinch joint

| S.no | Spot Pressure (bar) | Clinching Pressure (bar) | Weld Time (ms) | Squeeze Time (ms) | Hold Time (ms) | Peak Strength (ms) |
|------|---------------------|--------------------------|----------------|-------------------|----------------|--------------------|
| 1 | 4 | 6 | 900 | 400 | 250 | 2793 |

Table 13 Peel test result for clinch joint-assisted spot welding

| S.no | Clinching Pressure (bar) | Spot Pressure (bar) | Weld Time (ms) | Squeeze Time (ms) | Hold Time (ms) | Peak Strength (ms) |
|------|--------------------------|---------------------|----------------|-------------------|----------------|--------------------|
| 1 | 6 | 4 | 900 | 400 | 250 | 1736 |

As it is observed from the figure 39 (a) that failure mechanism of the joint was button failure and (b) maximum load carried by the joint was 2793 N.

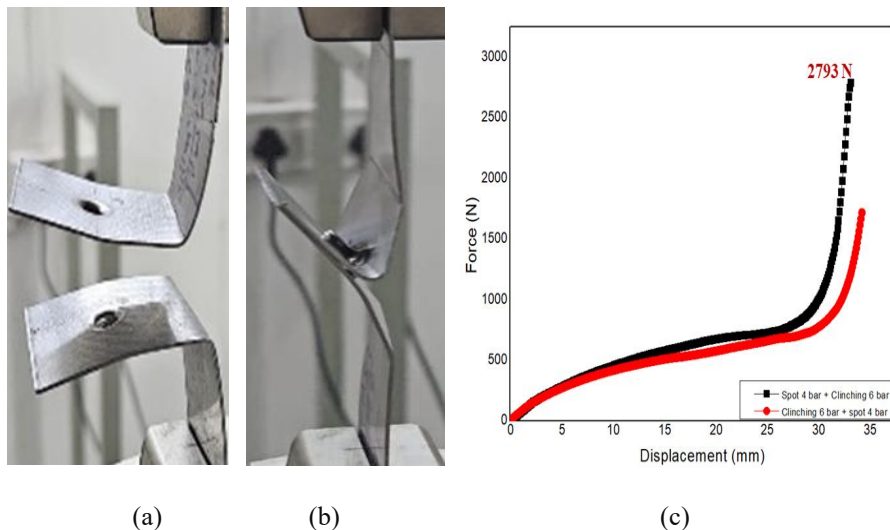


Figure 39 Failed sample after peel test (a) Spot welding assisted clinch joint
(b) clinching assisted spot welding (c) Result of the lap shear test.

5.2.6 Microstructure analysis of nugget formation in resistance spot welding.

The experiment was performed using RSW on the mild steel sheets to analyse the changes in the microstructure behaviour, each has a 0.8 mm thickness. Further, the welded sample was cold-mounted to preserve the structure for examination. Initially, for sample preparation, the surface was polished using different grades of sandpaper, finishing with a diamond polishing pad to get a smooth, mirror-like finish. The polished surface was then etched using a Nital solution, which helps reveal the internal structure of the material. The figure 39 shows a full cross-section of the welded area. Key features such as the fusion zone, heat-affected zone (HAZ), nugget width (3.39 mm), penetration depth (0.48 mm), and indentation depth are labeled. This overview gives a clear idea of how heat affected the different regions during welding.

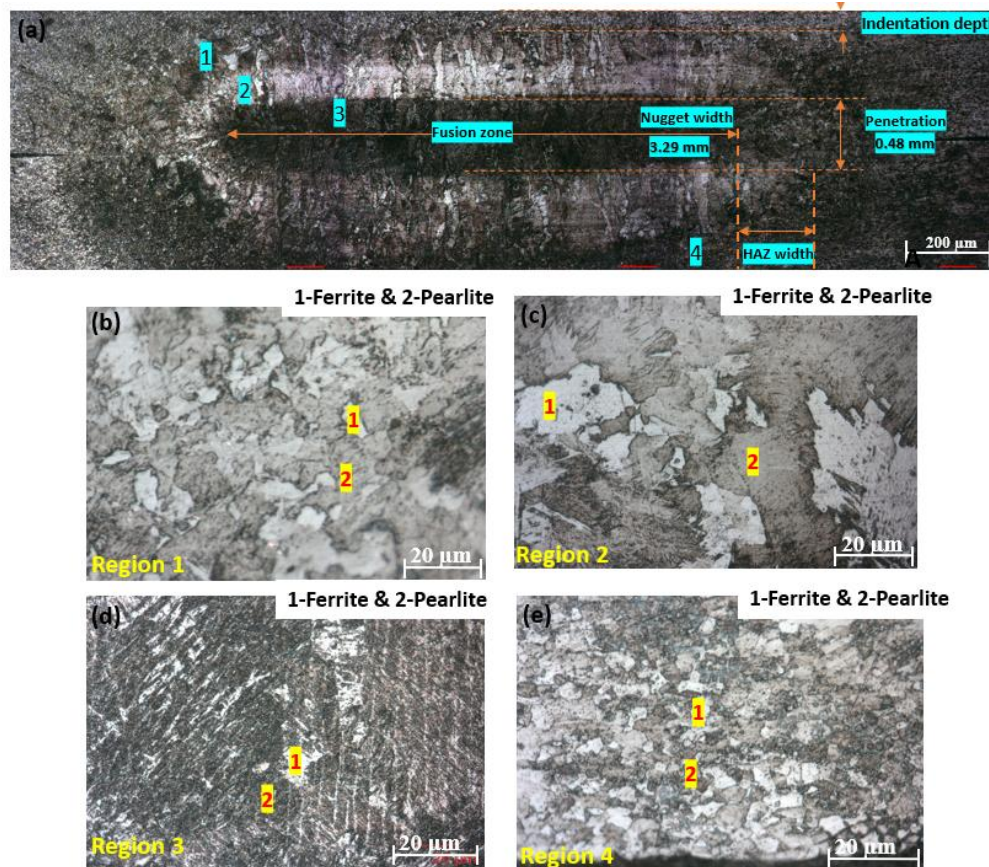


Figure 40 (a) Mild steel sheet nugget zone (b) base metal (c) Near HAZ (d) Fusion zone (d) Opposite of heat affected zone

To study the microstructure in more detail, four region marked on the image (1,2,3,4) were examined under a microscope at 500x magnification. Below are the detailed study of figure 39.

➤ Image (b) – Region 1 (Base Metal)

This area is far from the weld and shows the original structure of mild steel. It contains a mix of ferrite (1) and pearlite (2)—ferrite appears lighter and softer, while pearlite is darker and harder.

➤ Image (c) – Region 2 (Near the HAZ)

This zone is close to the welding area and has been affected by heat. The structure is still ferrite and pearlite, but some grain growth is visible, showing that the material was exposed to high temperatures without melting.

➤ Image (d) – Region 3 (Fusion Zone)

This is the center of the weld where the material melted and re-solidified. The microstructure here looks different more like a cast structure with irregular, larger

grains showing it went through complete melting during welding.

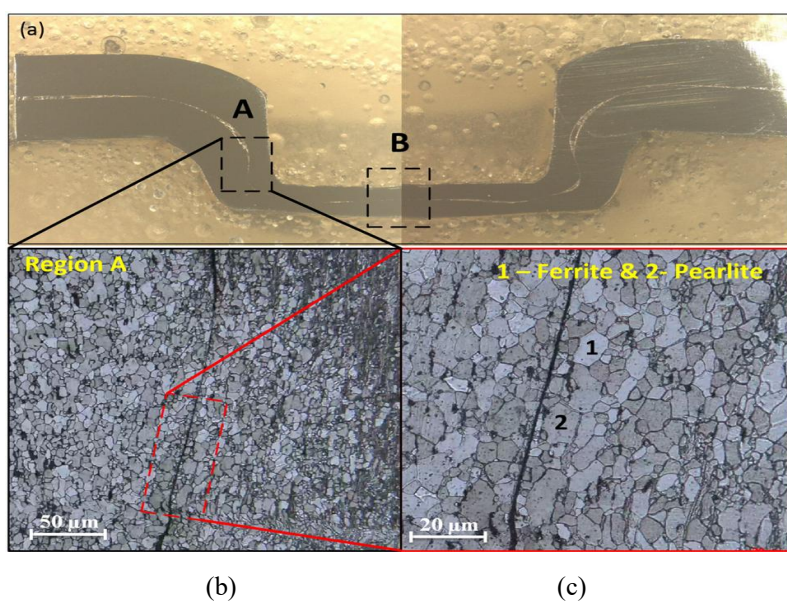
➤ **Image (d) – Region 4 (HAZ on the other side)**

Similar to Location 1, this area lies outside the heat-affected zone on the opposite side. It also shows an unchanged structure of ferrite and pearlite, confirming it remained unaffected by the welding heat.

This analysis helps us understand how the welding process changes the material's internal structure, which affects the strength and quality of the weld.

5.2.7 Microstructure analysis on the effect of clinching-assisted RSW

The cross-sectional view and corresponding optical microscope images of the clinching-assisted RSW joint are shown in Figure 41 (a). A cross-sectional view of the joint is shown in Figure 41 (b). Two regions were selected for further analysis: one is the neck thickness region marked as Region A, and the other is the bottom thickness region marked as Region B, as shown in Figure 41 (a). Microscopic analysis of the bottom thickness region was performed, and the same is shown in Figure 41 (b). Microscopic analysis of the neck thickness region was performed, and the same is shown in Figure 41 (c). Grain flow pattern was observed in the microscopic image of the neck thickness region. Enlarged microscopic views of the neck thickness region are shown in Figure 41 (d) and Figure 41 (e). Ferrite and Pearlite structure was observed in the microscopic images of the neck thickness region when observed at a scale of 50x or 20 μm .



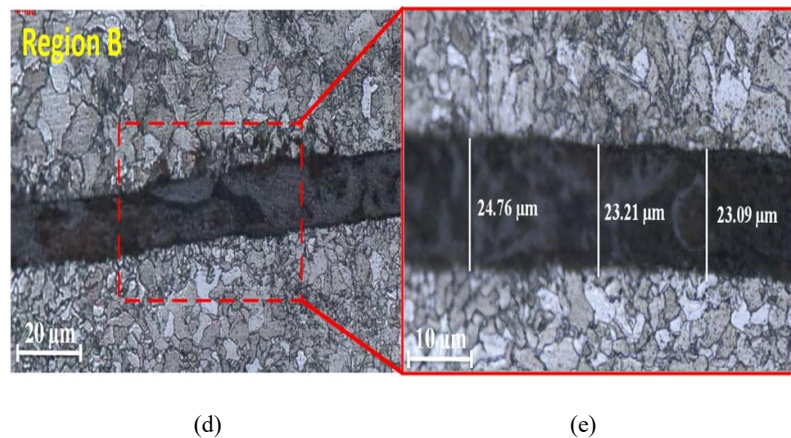


Figure 41 (a) Cross-sectional view of clinching assisted RSW, (b) 20x – 50 μm (scale), (c) 50x – 20 μm (scale), (d) 50x – 20 μm (scale), and (e) 100x – 10 μm (scale)

5.2.8 Microstructure analysis on the effect of RSW-assisted clinching

The cross-sectional view and corresponding optical microscope images of the RSW-assisted clinch joint are shown in Figure 42. A cross-sectional view of the joint is shown in Figure 42 (a). Two regions were selected for further analysis: one is the neck thickness region marked as Region A, and the other is the bottom thickness region marked as Region B, as shown in Figure 42 (a). Microscopic analysis of the neck thickness region was performed, and the same is shown in Figure 42 (b). Enlarged microscopic views of the neck thickness region are shown in Figure 42 (c). Ferrite and Pearlite structure was observed in the microscopic images of the neck thickness region when observed at a scale of 50x or 20 μm , as shown in Figure 42 (c). A microscopic view of the bottom thickness region is shown in Figure 42 (d). A gap was observed at the interface in the region, and it was also measured, the same is shown in Figure 42 (e).

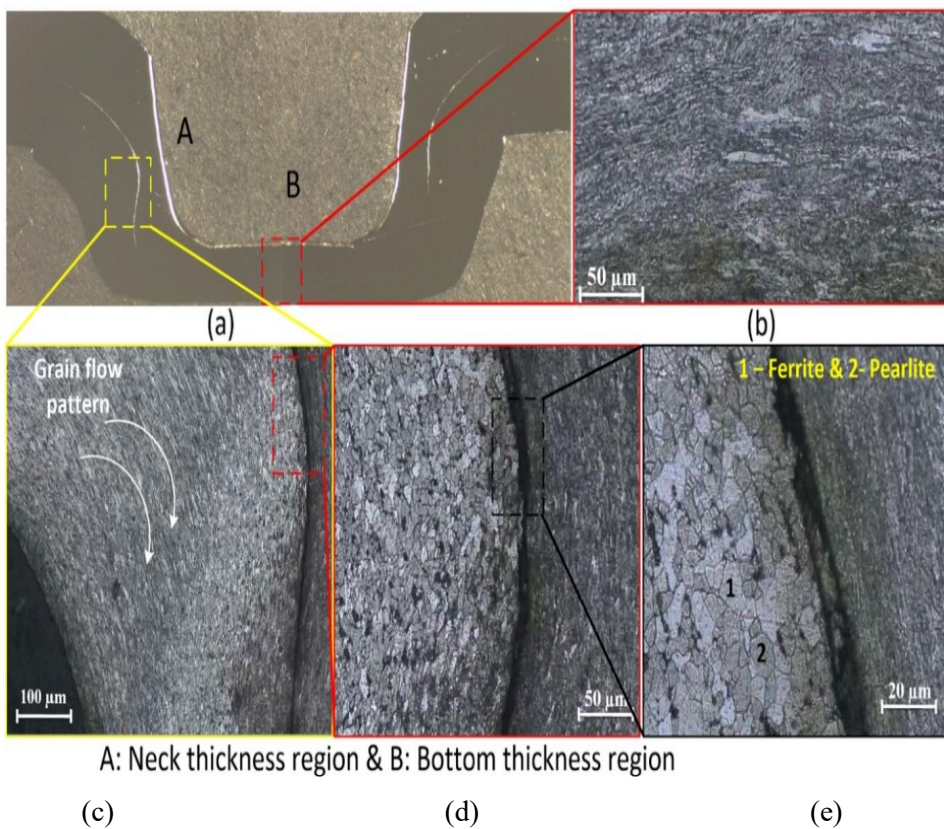


Figure 42 (a) Cross-sectional view of RSW assisted clinch joint, (b) 20x – 50 μm (scale), (c) 50x – 20 μm (scale), (d) 50x – 20 μm (scale), and (e) 100x – 10 μm (scale)

5.2.9 Scanning electron microscopy analysis

SEM images of the clinching-assisted RSW of the samples are shown in Figure 43. Two different regions were selected for the study. One is the bottom thickness region, and the other is the neck thickness region. SEM image of the clinching bottom thickness region and its enlarged view is shown in Figure 43 (a) and Figure 43 (b). SEM image of the clinching neck thickness region and its enlarged view is shown in Figure 43 (c) and Figure 43 (d).

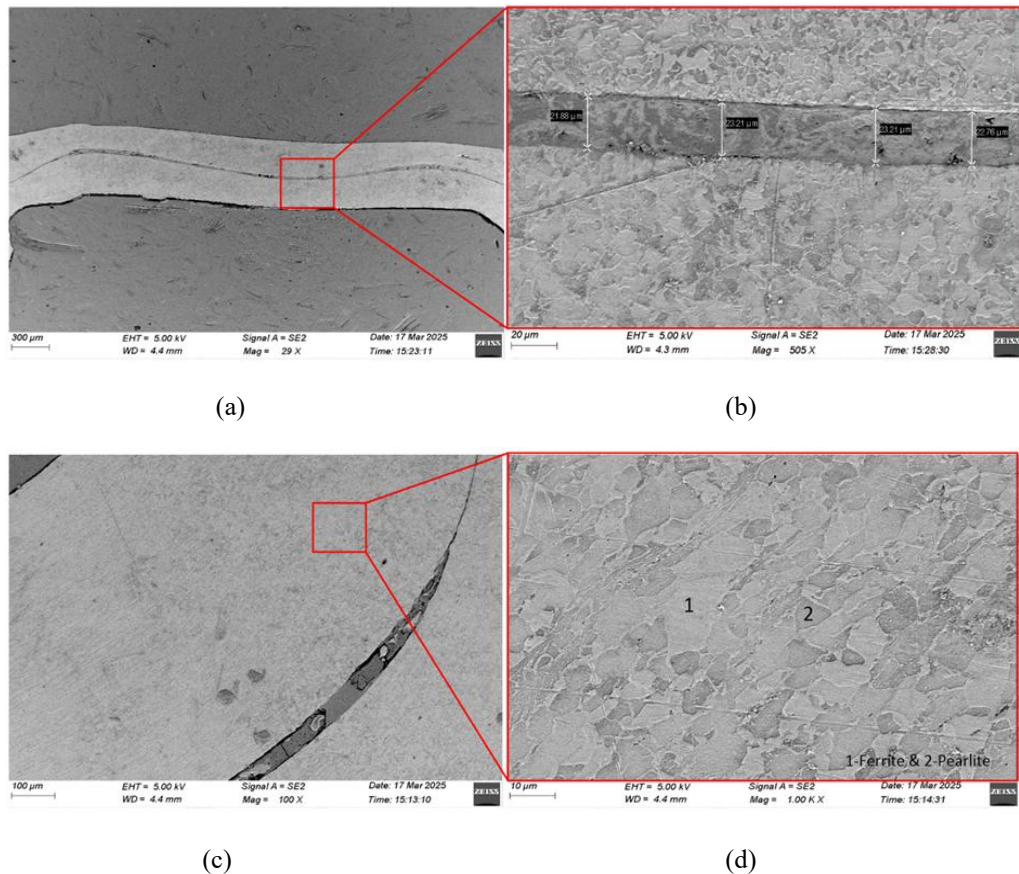


Figure 43 View of Clinching assisted RSW (a) Clinching bottom thickness region, (b) Enlarged view of clinching bottom thickness region region, (c) Clinching neck thickness region, and (d) Enlarged view of clinching neck thickness region

SEM images of the RSW-assisted clinch joint of the samples are shown in Figure 44. Two different regions were selected for the study. One is the bottom thickness region, and the other is the neck thickness region. SEM image of the clinching bottom thickness region and its enlarged view is shown in Figure 44 (a) and Figure 44 (b). SEM image of the clinching neck thickness region and its enlarged view is shown in Figure 44 (c) and Figure 44 (d).

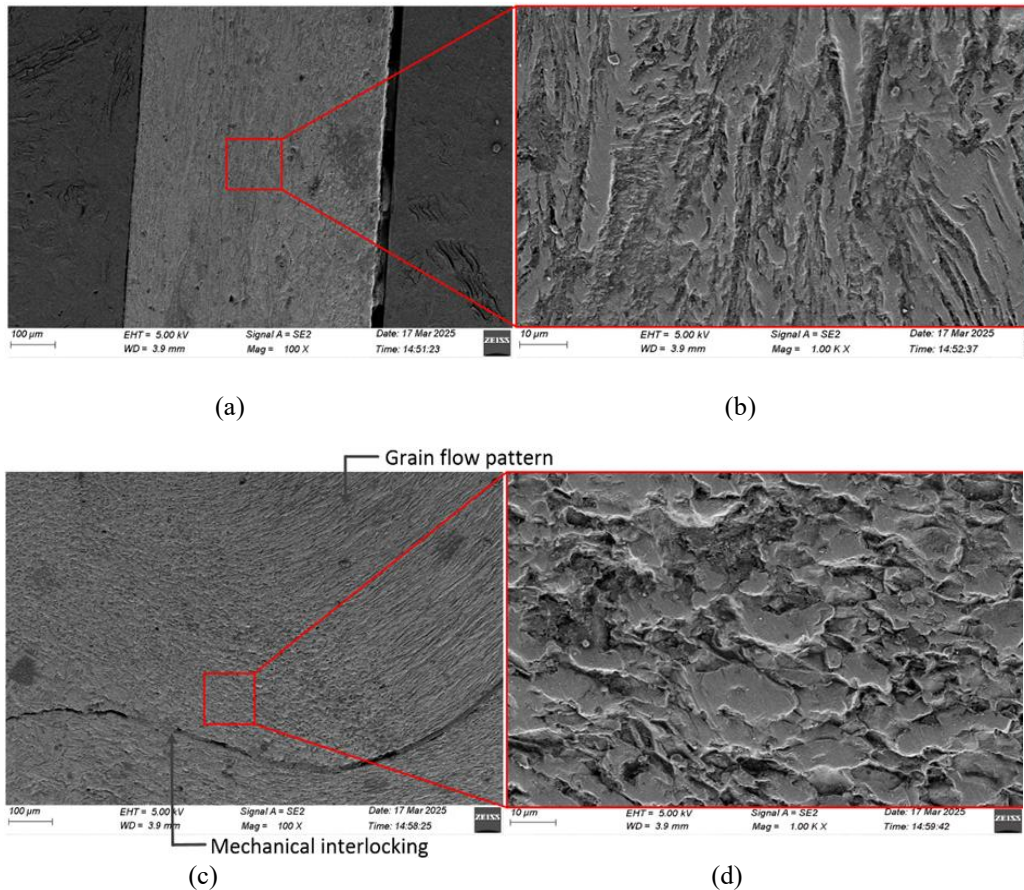


Figure 44 View of RSW-assisted clinch joint (a) Clinching bottom thickness region, (b) Enlarged view of clinching Clinching bottom thickness region, (c) Clinching neck thickness region, and (d) Enlarged view of clinching neck thickness region

5.2.10 Energy dispersive spectroscopy analysis on two sheet spot welding.

To understand what elements are present in the joint area after welding and clinching. Energy Dispersive Spectroscopy was performed on the bottom thickness area of the spot welding-assisted clinched region between two mild steel sheets. The SEM image shown in the Figure 45 (a) is the exact area we analyzed. The EDS results showed a high amount of iron (Fe) and a small amount of carbon (C), which matches the normal composition of mild steel.

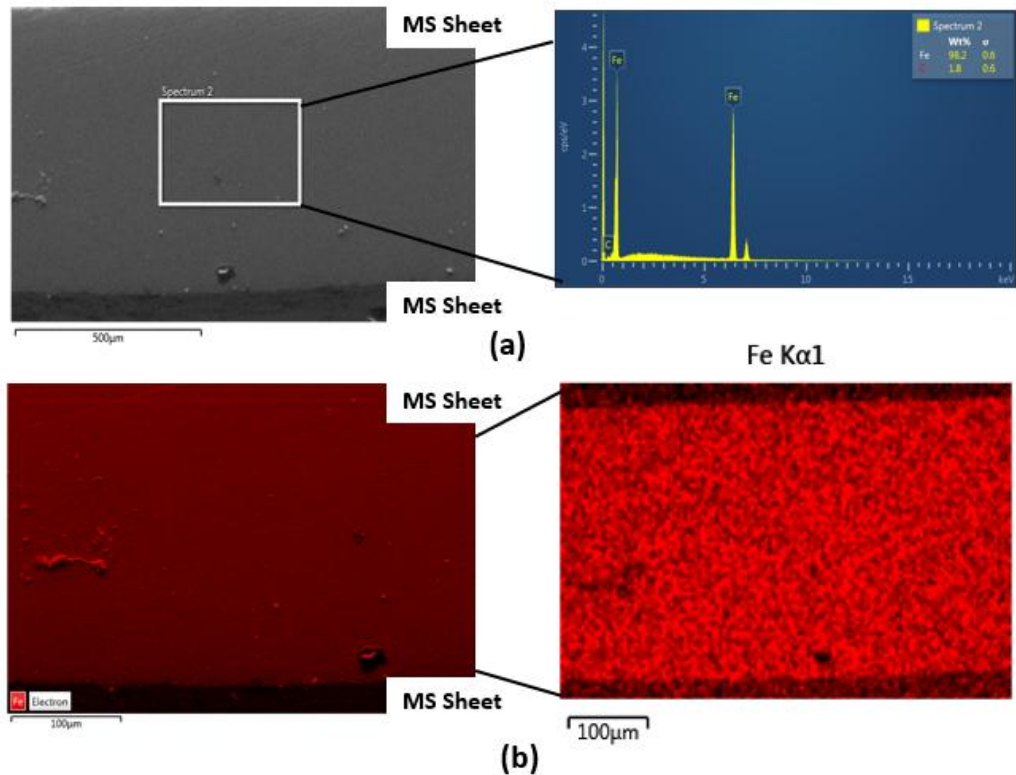


Figure 45 EDS analysis on (a) area of two sheet spot welding assisted clinching (b) mapping of two sheet spot welding assisted clinching

EDS mapping was used to see in Figure 45 (b) how iron is spread across the joint area. The Fe K α 1 map shows that iron is evenly distributed, which means the materials joined well during the clinching and welding process. This even distribution is important for the strength and quality of the joint.

5.2.11 Numerical analysis of spot welding on three 0.8 mm SS-MS-GI sheets.

The simulation results, as shown in Figure 46, efforts were made to analyze the temperature behavior during RSW of a three-layer dissimilar steel stack comprising SS on the top, MS in the middle, and GI at the bottom. Despite this, the recorded temperature remained almost unchanged throughout the process and failed to reach the melting point required for proper weld nugget formation. This outcome suggests limitations in the thermal-electrical interaction within the model, possibly due to insufficient heat generation arising from inadequately defined electrical resistance or boundary inputs. Consequently, the simulation did not exhibit the expected localized heating and nugget formation typically seen in experimental results. To enhance the accuracy of future simulations, it is essential to fine-tune material definitions, interface resistances, and thermal boundary conditions for better representation of heat distribution and fusion during the welding process.

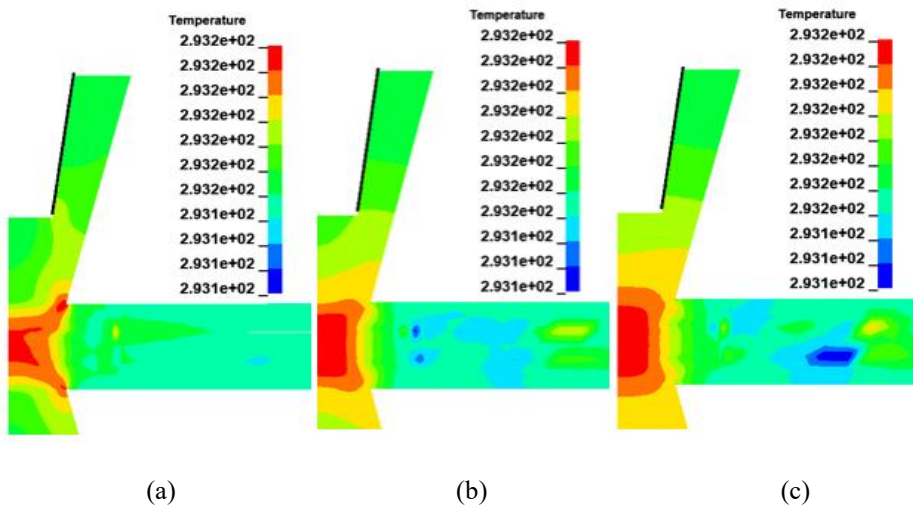


Figure 46 Fringe pattern of three dissimilar steel sheet nugget formation

The current density pattern depicted in Figure 47 investigated the distribution of current density during RSW of a three-layer dissimilar steel stack consisting of SS on the top, MS in the middle, and GI at the bottom. Under ideal conditions, higher current density is expected at the electrode-sheet contact point and at the interfaces between the sheets, facilitating localized heating necessary for weld nugget formation. However, in the current model, the current density exhibited minimal spatial variation and failed to concentrate in the weld zone as anticipated.

This uniform behavior indicates limitations in the electrical setup of the simulation, potentially due to insufficient definition of contact resistance, boundary conditions, or applied electrical load. As a consequence, the model did not generate the localized heat required for effective bonding. To improve future simulations, it is recommended to carefully reassess the electrical boundary parameters, refine contact resistance settings, and ensure accurate material property definitions to achieve realistic current flow and corresponding thermal effects.

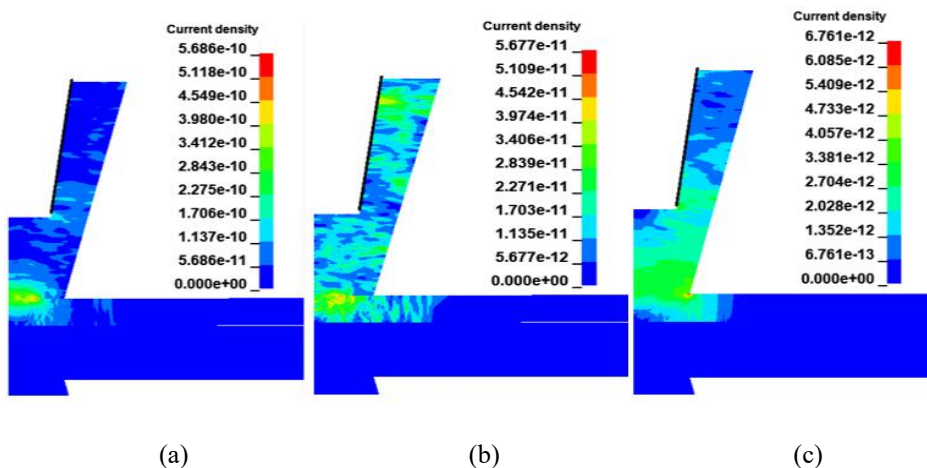


Figure 47 Fringe pattern of three dissimilar steel sheet current density variation

5.2.12 Numerical analysis of spot welding on two 0.8 mm MS sheets.

The simulation results in Figure 48 show that as the welding process progresses, heat concentrates at the interface between the two mild steel sheets. This causes the temperature in that region to rise significantly, eventually reaching the melting point of the material. As a result, a weld nugget is formed between the sheets, which indicates successful joining due to localized melting and fusion. The temperature of the weld nugget was around 1750 K.

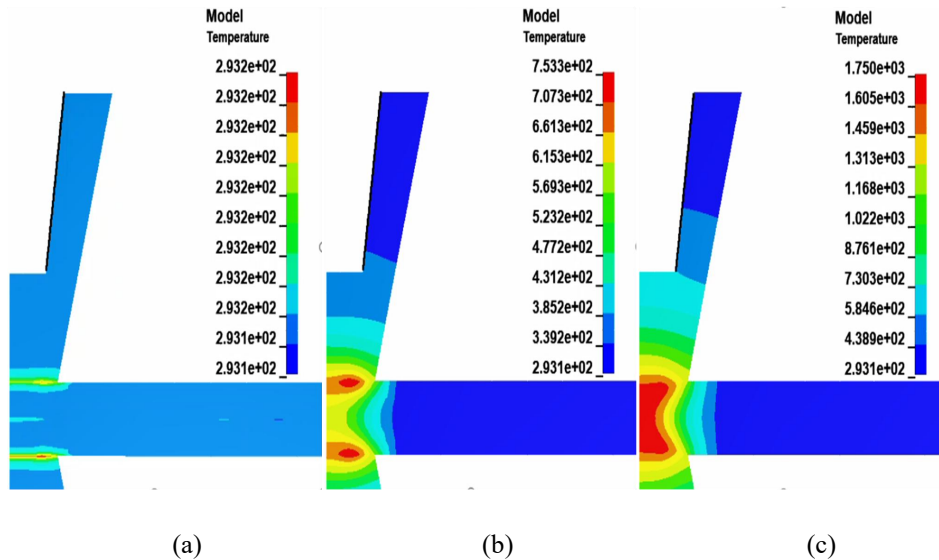


Figure 48 Fringe pattern of two mild steel sheet nugget formation

The current density distribution in Figure 49 shows a higher concentration of current at the contact area between the electrode and the top sheet, and at the interface between the two sheets. This concentrated flow of current generates localized heat due to electrical resistance, leading to nugget formation. As time progresses, the current density spreads slightly but remains focused at the weld zone, ensuring proper heating and joint formation. The maximum value of current density is 1226 A/mm^2 .

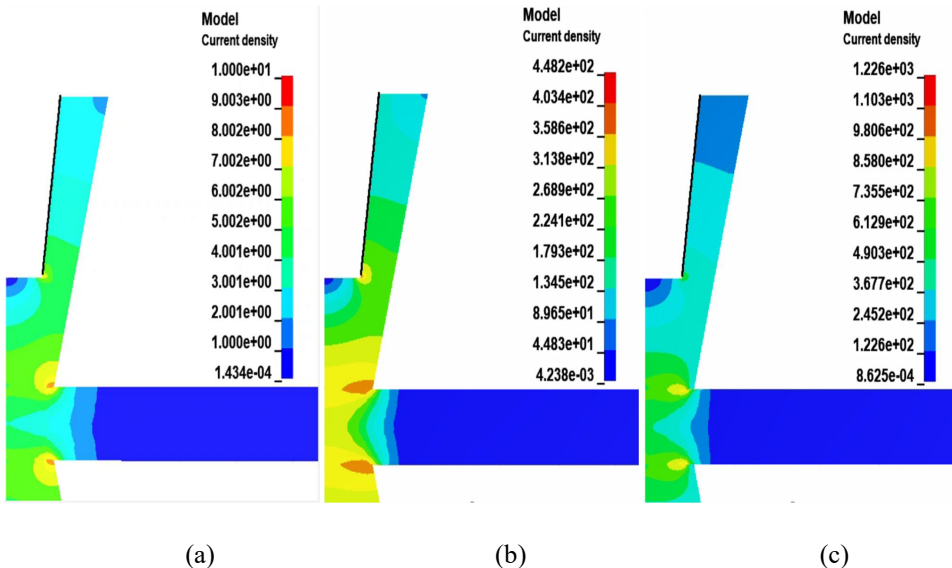


Figure 49 Fringe pattern of two mild steel current density variation

5.2.13 Numerical analysis of mechanical clinching on two 0.8 mm MS sheets.

During the mechanical clinching process, shown in Figure 50 (a) the effective plastic strain in the two mild steel sheets increased as the punch moved downward and deformation occurred.

- (1) Initial stage (start):- The effective plastic strain was 0 (no deformation).
- (2) Final stage (end):- The maximum plastic strain reached around 1.989 (unitless) which was concentrated near the neck and interlock region where the sheets experienced maximum plastic deformation.

This indicates that significant material flow and forming occurred in those areas to create the clinch joint.

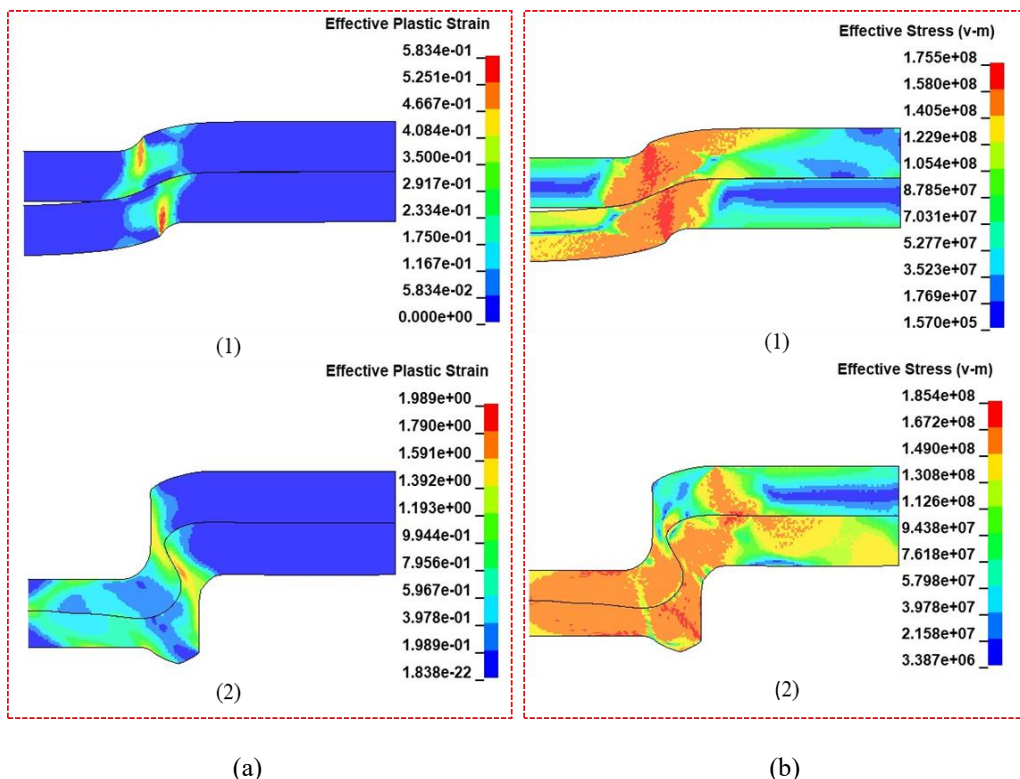


Figure 50 Fringe pattern (a)Two mild steel sheet plastic strain variation (b) Two mild steel sheet von-mises Stress variation

From figure 50 (b) effective stress (Von Mises stress) also increased as the punch compressed the sheets, causing deformation and material flow.

- (1) Initial stage (start):- The effective stress was around 0.157 MPa.

(2) Final stage (end):- The maximum Von Mises stress reached 185.4 MPa. mainly concentrated in the neck and contact zones, where the material was highly stressed due to the clinching force.

These results confirm that both stress and strain peaked in the joint formation zone, which is expected during a successful clinching process.

Chapter 6

Conclusion and future directions

This chapter presents the key conclusions derived from a comprehensive investigation on joining sandwich structures consisting of SS304, MS1006, and GI. It also includes an evaluation of MS1006–MS1006 joints using both resistance spot welding and clinching methods. The chapter presents the study's results, underlining their practical relevance and the value of the conclusions drawn. It also explores potential real-life applications and proposes areas for future investigation within this field.

6.1 Summary of findings

The experimental procedures and research methodology, detailed in Chapter 3 outlines the experimental setup and research methods, while Chapter 5 presents the findings related to the joining of SS304, MS1006, and GI sheets through resistance spot welding. The study also explores the joining of MS1006–MS1006 sheet pairs using both mechanical clinching and resistance spot welding techniques. Based on the experimental results and analyses, the following key conclusions have been drawn.

- For the three-layer spot welding process, the best parameters found were a welding pressure of 4 bar and a weld duration of 700 milliseconds, with the sheet arrangement having SS304 on the upper layer, MS1006 in the center, and GI at the bottom. This setup resulted in the highest lap shear test strength of **11776 N** and a maximum peel load of **236 N**.
- Three stack from the microstructural study, in the clinch-assisted spot welding, the material is not fused properly at the bottom thickness region, whereas in the case of the spot welding-assisted clinching joint, the materials were fused properly.
- For two-stack joining of MS1006–MS1006 using both spot welding and clinching, the clinching process achieved the highest strength of **2039 N** at an optimized pressure of **6 bar**, while spot welding produced a superior joint strength of **6071 N**.

with a welding pressure of **4 bar** and a weld time of **900 milliseconds**.

- The performance of two hybrid joining techniques was evaluated. **Spot welding-assisted clinching** demonstrated superior strength, achieving a maximum lap shear load of **6100 N** and a maximum peel load of **2793 N**. In comparison, clinching-assisted spot welding reached a maximum lap shear load of **2015 N** and a maximum peel load of **1736 N**. Overall, the lap shear and peel tests showed that spot welding-assisted clinching provided better joint strength than clinching-assisted spot welding for the mild steel-mild steel (MS-MS) sheet combination.
- From the microstructural study, in the clinch-assisted spot welding, the material is not fused properly at the bottom thickness region, whereas in the case of the **spot welding-assisted clinching joint**, the materials were fused properly.
- Numerical simulations on three-sheet showed a nugget temperature of and for two-sheet mild steel welding showed a nugget temperature of 1750 K. In clinching, the neck thickness and interlock were evaluated, with von Mises stress reaching 185 MPa.

6.2 Implications and Significance

This research highlights how combining SS304, MS1006, and GI sheets can result in strong and durable joints suitable for practical use. It shows that each material brings its own benefits such as SS304 imparts corrosion resistance, MS1006 strength and formability, and GI has cost-effectiveness which makes them a valuable combination in areas like car manufacturing, home appliances, and sheet metal structures.

Further, the study also helps compare two common joining methods: spot welding and clinching. While spot welding creates stronger joints, clinching is useful when the surface coating of materials needs to be preserved. These findings are important for designers and engineers, as they help choose the most effective and material-friendly joining method depending on the product requirements and design constraints

6.3 Limitations and Future Research

While the study provides useful insights into the joining of three dissimilar sheets using resistance spot welding and the combination of clinching with spot welding for two-sheet joints, there are still some limitations that need to be addressed.

Spot welding and clinching are simple and cost-effective, but they struggle with complex or curved joints. Future research can investigate improved fixtures or custom electrode and die designs to make these methods usable in such cases instead of switching to other techniques.

Another limitation is challenge in fully understanding how the nugget forms and how the material flows during spot welding and clinching, even with experiments and simulations. This makes it harder to accurately link microstructural changes to the final joint strength. remove limitations

For future research, a broader set of parameters can be tested to better understand their effects on joint quality and strength. Advanced imaging techniques like SEM-EBSD can be used to examine internal defects, nugget shape, and interfacial bonding. Exploring other material combinations, joint configurations, and hybrid joining processes can also help improve performance in automotive or structural applications.

6.4 Recommendations for further study

Based on what this study has shown, and the challenges faced, the following points are suggested for future research on three-sheet resistance spot welding (RSW) and two-sheet hybrid clinching combined with spot welding

(a) Better ways to study nugget formation

It's still difficult to fully understand how the weld nugget forms and how the material flows during welding and clinching, especially with the tools currently available. Future research could use modern technologies like real-time thermal cameras, high-speed video, or built-in sensors to study these changes as they happen. This would help give a clearer picture of how the joint develops and behaves.

(b) Exploring hybrid joining methods

Using spot welding along with other joining techniques like clinching or adhesives might help improve joint strength and performance. More research is needed to study how different combinations work together, including which method should be done first and how different materials respond to them.

(c) Adapting new materials

As industries start using stronger and lighter materials, such as high-strength steels and aluminium alloys, it's important to find out how well RSW and clinching work with them. Future studies should look at whether these techniques need to be adjusted or if new joining methods need to be developed to handle these materials effectively

REFERENCES

- [1] Kimchi, Menachem, and David H. Phillips. *Resistance Spot Welding: Fundamentals and Applications for the Automotive Industry*. Butterworth-Heinemann, 2020.
- [2] Wan, Xiaodong, Yuanyuan Wang, and Cuisia Fang. "Welding defects occurrence and their effects on weld quality in resistance spot welding of AHSS steel." *ISIJ International* 54.8 (2014): 1883-1889.
- [3] Shen, Jie, et al. "Modeling of resistance spot welding of multiple stacks of steel sheets." *Materials & Design* 32.2 (2011): 550-560.
- [4] Mishra, Debashish, et al. "Dissimilar resistance spot welding of mild steel and stainless-steel metal sheets for optimum weld nugget size." *Materials Today: Proceedings* 46 (2021): 919-924.
- [5] Zhou, Kang, et al. "Process optimization of aluminum/steel resistance spot welding based on dynamic resistance analysis." *Journal of Materials Science* 58.47 (2023): 17908-17929.
- [6] Zhang, Xizang, and Chao Chen. "Experimental investigation of joining aluminum alloy sheets by stepped mechanical clinching." *Journal of Materials Research and Technology* 19 (2022): 566-577.
- [7] Ren, Xiaoqing, et al. "Investigation on mechanical behavior of clinched joints produced with dissimilar dies." *Proceedings of the Institution of Mechanical Engineers, Part B: Journal of Engineering Manufacture* 237.1-2 (2023): 31-42.
- [8] Lei, Lei, et al. "Failure modes of mechanical clinching in metal sheet materials." *Thin-Walled Structures* 144 (2019): 106281.
- [9] Zhou, Kang, et al. "Process optimization of aluminium/steel resistance spot welding based on dynamic resistance analysis." *Journal of Materials Science* 58.47 (2023): 17908-17929.
- [10] Abe, Y., T. Kato, and Kenichiro Mori. "Joining of aluminum alloy and mild steel sheets using mechanical clinching." *Materials Science Forum*. Vol. 561. Trans Tech Publications Ltd, 2007.
- [11] Kamble, Pritam, and Rayappa Mahale. "Simulation and parametric study of clinched joint." *Int Res J Eng Technol* 3.05 (2016): 2730-2734.
- [12] Kang, Hong-Tae, et al. "Fatigue performance of resistance spot welds in three sheet stack-ups." *Procedia Engineering* 2.1 (2010): 129-138.

[13] Pasarkar, A., et al. "Review of fatigue behavior of resistance spot welds." *Res. Eng. Struct. Mater* 9 (2023): 181-194.

[14] Zhang, Yu, et al. "Joining aluminum alloy 5052 sheets via novel hybrid resistance spot clinching process." *Materials & Design* 118 (2017): 36-4

[15] Panagiotis Stavropoulos & Kyriakos Sabatakaki "Quality Assurance in Resistance Spot Welding: State of Practice, State of the Art, and Prospects.", doi.org/10.3390/met14020185

[16] Marwah S.Fakhria,Ibtihal A. Mahmoodb,Ahmed Al-Mukhtarc "The electrical and mechanical aspects of aluminum and copper resistance spot weld joints", doi10.30684/etj.2023.143734.1606

[17] Milan Brožek, Alexandra Nováková, Ota Niedermeier "Resistance spot welding of steel sheets of the same and different thickness", doi:10.11118/actaun201765030807

[18] Ahmet Hasanbasoglu,Ramazan Kacar "Resistance spot weldability of dissimilar materials ", doi.org/10.1016/j.matdes.2006.05.013

[19] M. Ullrich1, M. Wohner1 & S. Jüttner "Quality monitoring for a resistance spot weld process of galvanized dual-phase steel based on the electrode displacement", doi.org/10.1007/s40194-024-01720-w

[20] Haiqiang Long , Yumei Hu, Xiaoqing Jin , Jinhua Shao , Hao Zhu "Effect of holding time on microstructure and mechanical properties of resistance spot welds between low carbon steel and advanced high strength steel", doi.org/10.1016/j.commatsci.2016.01.011

[21] Sushree Shefali Mishra "Research on Resistance Spot Welding of Dissimilar Metal Sheets: An Overview"

[22] Keke Yang et al. "Expulsion prevention in resistance spot welding of dissimilar joints with ultra-high strength steel: An analysis of the mechanism and effect of preheating current", doi.org/10.1016/j.jmapro.2024.06.034

[23] Zhigang Hou, et al. "Finite element analysis for the mechanical features of resistance spot welding process", doi.org/10.1016/j.jmatprotec.2006.03.143

[24] Sun, H. T., et al. "Effect of variable electrode force on weld quality in resistance spot welding." *Science and Technology of Welding and Joining* 12.8 (2007): 718-724.

[25] Chu, Mingming, et al. "Clinching of similar and dissimilar sheet materials of galvanized steel, aluminium alloy and titanium alloy." *Materials Transactions* 59.4 (2018): 694-697.

[26] Fang, Xiangfan, and Fan Zhang. "Hybrid joining of a modular multi-material body-in-white structure." *Journal of Materials Processing Technology* 275 (2020): 116351.

[27] Muhammad Iqbal hafizi. "Resistance spot welding of stainless steel and mild steel."

[28] M. Pouranvari. Effect of Welding Parameters on the Peak Load and Energy Absorption of Low-Carbon Steel Resistance Spot Welds.

[28] Liu, Hui, Xue Dong Xu, and Xiao Qing Zhang. "Optimization of parameters and research on joint microstructure of resistance spot welding for 316 stainless steel." *Advanced Materials Research* 652 (2013): 2326-2329.

[29] Aravinthan, A., and C. Nachimani. "Metallurgical study of spot welds growth on mild steel with 1mm and 2mm thicknesses." *Journal-The Institution of Engineers, Malaysia* 72.4 (2011): 46-54.